

CFD Analysis of NACA 0012 Aerofoils: Examining the Impact of Varied Angles of Attack on Lift and Drag Coefficients

Eng. Esam Faleh Alajmi¹; Hadyan Ali Alajmi²

^{1,2}Specialist Trainer (B) in Public Authority for Applied Education and Training,
The University of Arab Academy for Science, Technology and Transport

Abstract:- As aircraft technology improves, it becomes more important to use the right blade design. Wings can be found on many things, like airplanes, drones, wind machines, and more. ANSYS 2023 Software has been employed for performing a fluent toolbox for CFD analysis upon a NACA 0012 to see what happens to the lift coefficient when the angle of attack is raised. The solver model performed is k-w turbulence simulation was used to look at shape that was made in ANSYS fluent. At a speed of 50m/s, different attack angles between 0° and 25° have been tested to find out the lift and drag coefficients. Raising the angle of attack has been seen to raise the lift coefficient at first, but after a certain angle, the flow separates, and as the angle of attack is raised even more, the lift coefficient begins to decrease. As the turbulence gets stronger, the eddies it creates cause the flow to start breaking away from the airfoil surface. The airfoil's lift coefficient goes down and its drag coefficient goes up at the same time, which makes it perform poorly. The 20° angle of attack has the best performance ratio of 4.53, which means it has the most lift compared to drag of all the angles that were assigned.

Keywords:- Aircraft Technology, CFD Analysis, ANSYS Software, A NACA 0012, Blade Design, Airfoil's Lift and Drag Coefficient, Performance Ratio, Angle of Attack.

I. INTRODUCTION

From the historic flights, when Wright Brothers flighted, to the contemporary boundary of aerospace engineering, people's search to conquer the skies has been noticeable by progress of technological in addition relentless revolution. Aerodynamic effectiveness besides the capability to control aircraft under various operational situations keep at the aviation developments heart. One considerable aerodynamic issue is flowing separation on wings of aeroplane, which influence stability and efficiency. This phenomenon, where the flow of air separated from the surface of wing, causes to undesirable aerodynamic increased drag in addition instability. Efficiently managing flow separation is crucial for enhancing the fuel efficacy in addition performance of aircraft, so making accurate wing design a basis of modern aerospace engineering [1] and [2].

The present and combination of Computational Fluid Dynamics (CFD) in airplane design over the past time have revolutionized the design and enhancing processes within the manufacturing of flying. The development of CFD has considered as a transformative tool that lets engineers to emulate complex fluid flows besides test properties of aerodynamic without needing to the logistical demands besides high costs of traditional wind tunnel testing. This transformative not only reduces costs of developmental but also speed up the cycle of processes of aircraft design. By influence CFD, designers can emulate and relieve issues linked to drag besides flow separation at the phases of design, enhancing the aircraft's aerodynamic performance over a several of operating situations [3].

Aerofoils count the elementary units of the wings of aircraft which are precisely calculated to get maximum lift with the least drag. This is a real and strong area of the wing, except total air and flight potential; the air brings hard effects by affecting the shape of the wing and the amount of the lift created. Aerofoils revolutions in design have cause wings that can keep longer time of flight while efficacies are higher values, which is benefit for both military and commercial flying. The NACA 0012 Aerofoils has been a topic of widespread research due to its versatile implementation in various flight managements and it's important in the aerodynamics fundamental researches [4].

This paper focuses on the technical on the NACA 0012 Airfoils, that compared the changes in Angels of attach and study its effect on the coefficients of drag and lift by using CFD analysis techniques. Accurate information regarding how these coefficients change with the attack angles is imperative in improving Airfoil's designs and enhances performance of aircrafts. Both drag and lift forces are critical in defining the airplane performance, its usage, impact it has on the environment, in addition the amount of fuel it will need. Higher drag means, more thrust and thus more fuel consumption which causes more carbon emission and operational cost [4] and [5].

The paper is best suited to analyse the challenges of these dynamics by utilising CFD in ANSYS software to decipher the behaviour of the NACA 0012 Aerofoils under various attack angles. Therefore, in examining these interactions the paper will aim to find the thresholds and

general trends as to where changes in the attack angle causes worse performance, and where it more than doubles it. It is such knowledge that can aid the progression of the new generations Aerofoils that would provide improved fuel performance, efficiency, and above all, minimal impacts on the environment.

Even in this understanding of Aerofoils model along with great technological expansion other than the great utilise of CFD simulation to forecast the aerodynamic behaviour, increasing the ratio of lift to drag especially in the higher value of attack angle is still one of the major issues in the aerodynamics. The control is important at certain critical phases of a flight like taking off and landing and therefore this optimization is significant in these stages. To address the concepts of decreased lift and increased drag effectively it is significant for the operational efficiency in addition the safety of the flight. This paper addresses these significant challenges

by quantitatively evaluating the effects of diverse attack angles on the aerodynamic forces effecting on the NACA 0012 Aerofoils, offering a scientific basis for designing more effective Aerofoils that can contribute to the sustainable development of the aviation engineering.

II. LITERATURE REVIEW

A. Airfoiled and Wing

The wing, a crucial aerodynamic element, produces lift as it moves throughout the air. Its planform, observed from an airplane top view, outlines the wing's shape. Differing from the wing, the aerofoil signifies a two-dimensional cross-section designed precisely to manage airflow to create lift. The optimal aerofoil shape differs relying on operational altitude and intended speed, but all are crafted to effectively manipulate generate lift and airflow [6]. The following figure represents the wing plan geometry:

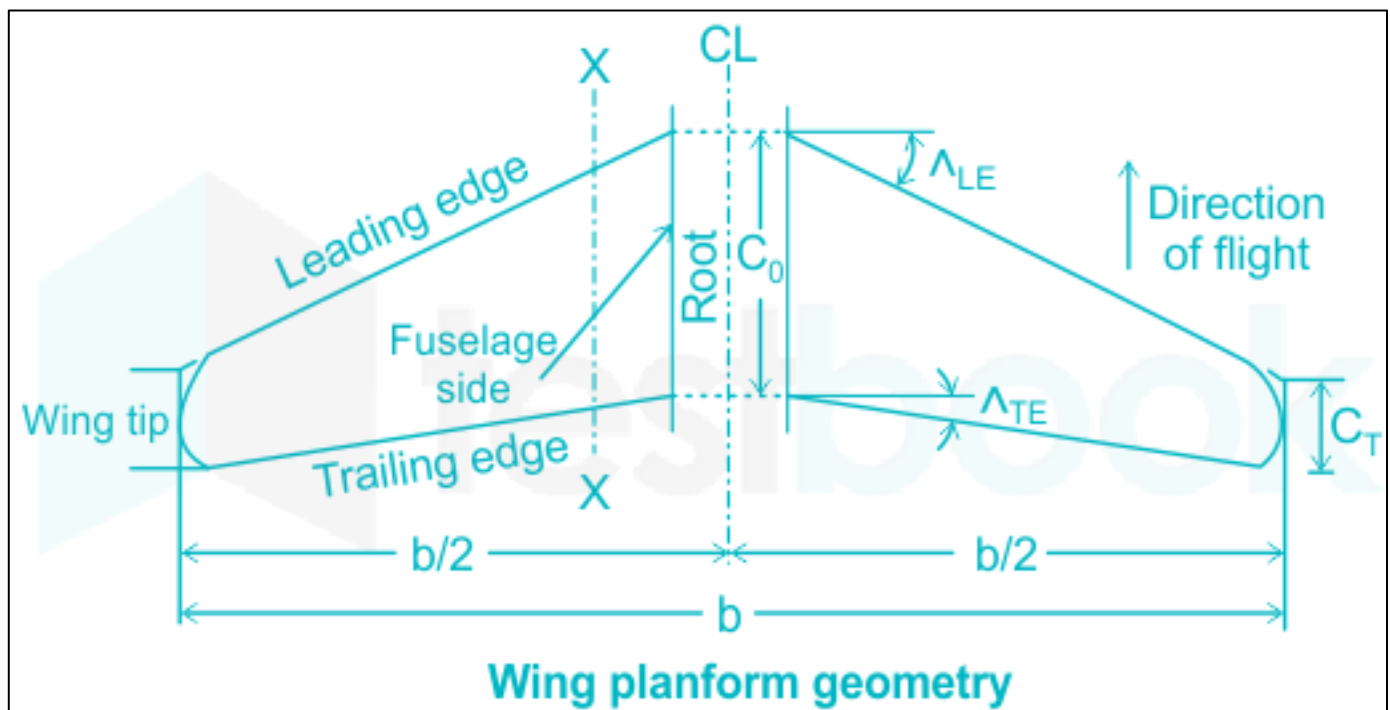


Fig 1: Geometry of Wing Plan [7].

When a horizontal wing is crossed by a vertical plane along the center-line, as revealed in X-X line, the cross-section formed is an airfoil. The chord line, running from trailing to leading edge, is central in defining airfoil features. It aids determine the camber line, the median contour between the wing's lower and upper surfaces, typically curved to enhance aerodynamic properties like lift. In symmetric airfoils, the shape is identical crossways the centerline, making the mean camber line align with the chord line, representing equidistant points along the chord from the

centerline. In asymmetric airfoils, the camber line turns from the chord line to enhance aerodynamics at various angles of attack.

The figure above labels essential components like wing tip, trailing and leading edges, wingspan dimensions ($b/2$), and centerline (CL), crucial for studying and improving wing aerodynamics. The following figure illustrates the airfoil geometry cross-section:

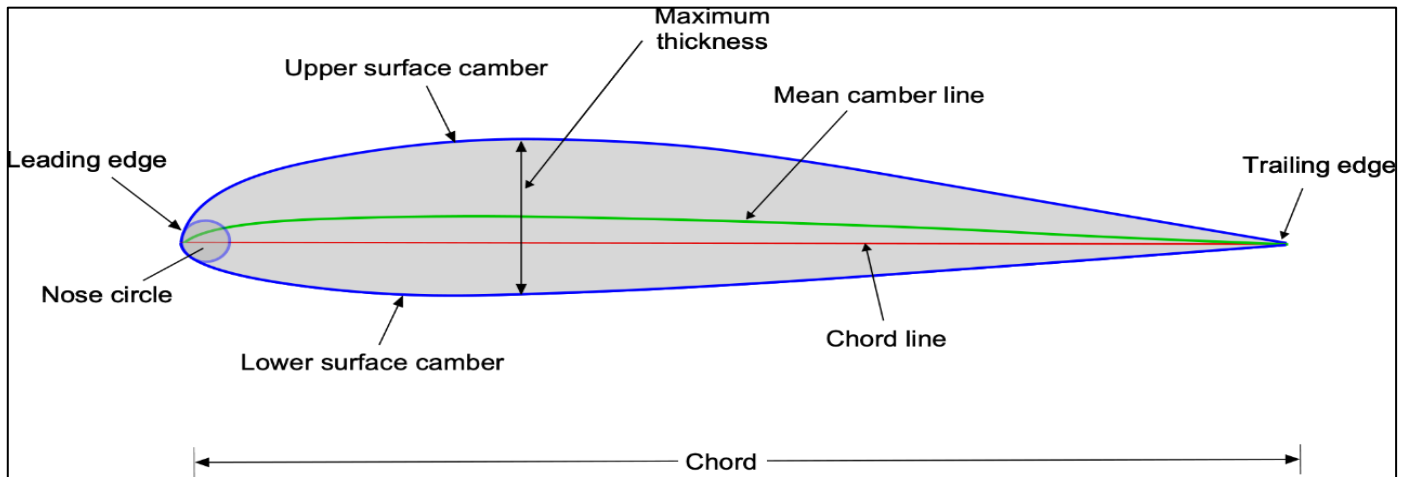


Fig 2: Geometry of Airfoil [8].

The figure above relates to airfoil where displays the cross section of the airfoil which is important in the designing of the airfoil. The chord line which is assumed together with the thickness of the blade as located at the bottom changes from the leading edge to the trailing edge of the airfoil recognizing the length of the airfoil. This line is fundamental for measuring the airfoil's geometric properties. The green curve signifies the mean camber line, which is the place of point's midway between the lower and upper surfaces and shows the curvature of the airfoil. This curvature or camber is vital for aerodynamic lift, inducing how air moves over the airfoil to produce lift efficiently. The arrows perpendicular to the chord line measure the airfoil maximum thickness, which affects its aerodynamic performance and characteristics such as lift and drag behavior.

B. Aerodynamic forces generated by an airfoil

Airplanes work in three dimensions, maneuvering around lateral, longitudinal, and vertical axes. The forces of thrust, drag, weight, and lift impact all aircraft during flight. Mastery of these forces through flight and power controls is crucial for dealing flight dynamics. This section explores

aerodynamics in aviation discussing how factors such as design, load factors, weight, and gravity influence an aircraft during different maneuvers [9]:

- Thrust represents the forward force from the propeller and engine, countering drag and aligned with the longitudinal axis.
- Drag represents the resisting force caused by the airflow aircraft's disruption, acting opposing and rearward thrust.
- Lift is produced by the dynamic interaction of air with the airfoil, directed perpendicular to the counteracting weight and flight path.
- Weight represents the downward force because of gravity, combining the aircraft's mass with its contents, opposing lift.

In steady flight, these forces balance as per Newton's Third Law, ensuring no unbalanced forces during climbing, level, or descending flight. Figure below represents the forces exerted on an aircraft during flight:

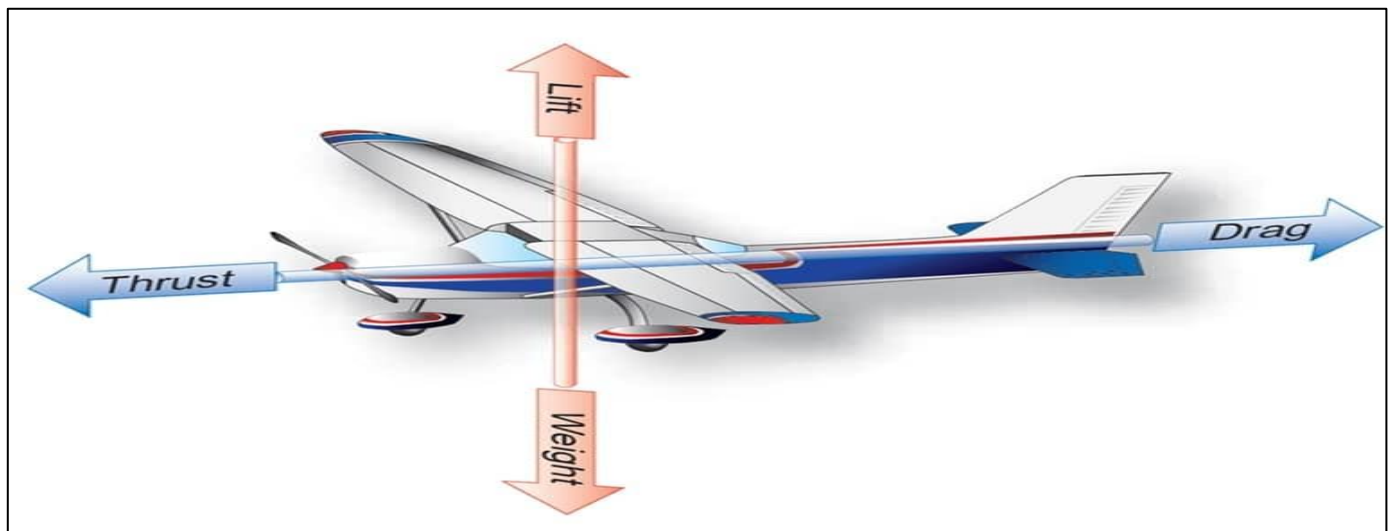


Fig 3: Forces Exerted on an Aircraft During Flight [10].

The concept that the four forces thrust, weight, lift, and drag are balanced does not suggest they are individually equal but that they neutralize each other's effects. For instance, in Figure 3, whereas these forces appear equal, they are actually counteracting one another. Another critical aerodynamic

principle is the angle of attack (alpha), which has been critical in understanding airplane performance, control, and stability since the advent of flight. The alpha is defined as the sharp angle between the airfoil's chord line and the relative wind direction [11], as depicted in Figure 4:

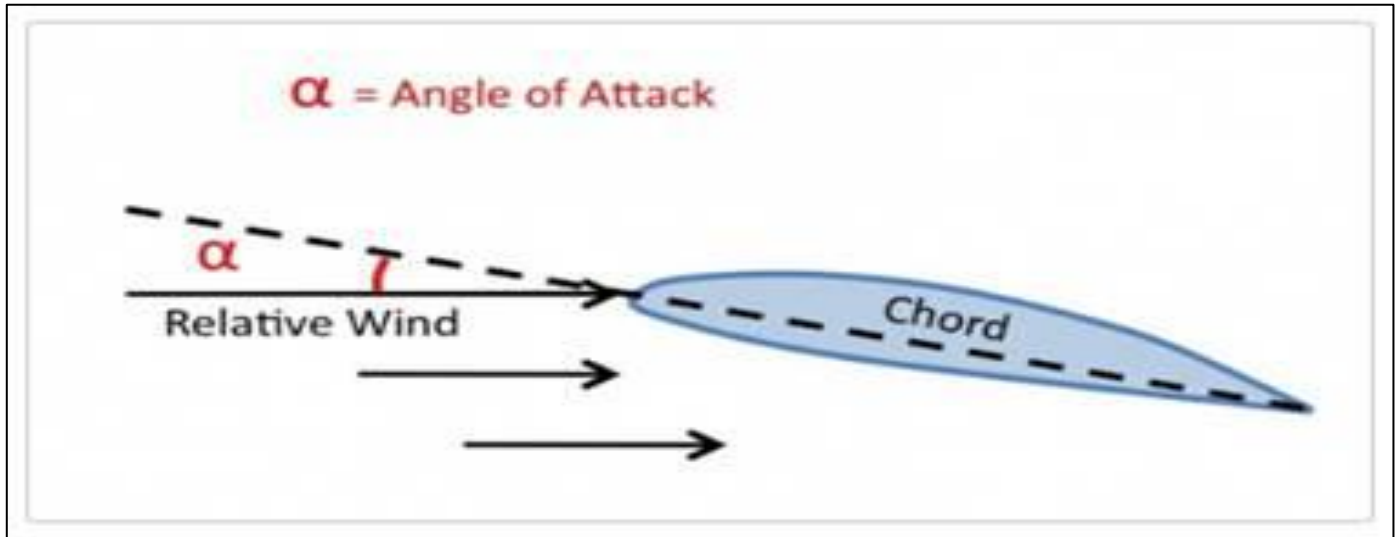


Fig 4: Angle of Attack Through Flight [12].

Pressure distribution measurements are critical through flight testing of flight research programs and new aircraft designs. These measurements confirm numerical validate and predictions any wind tunnel tests conducted, confirming that the aircraft works within safe structural load limits. Additionally, understanding air pressure distribution allows for accurate calculation of flight loads, confirming the aircraft's structural integrity under different operational conditions [13].

This research primarily explores the lift force produced by variations in air pressure. In steady-state flight, an aircraft's lift counterbalances its weight, whereas in powered flight, the aircraft's thrust offsets the drag. The forces exerted on an aircraft by air are considered into shear forces and pressure forces [14], as depicted in Figure 5:

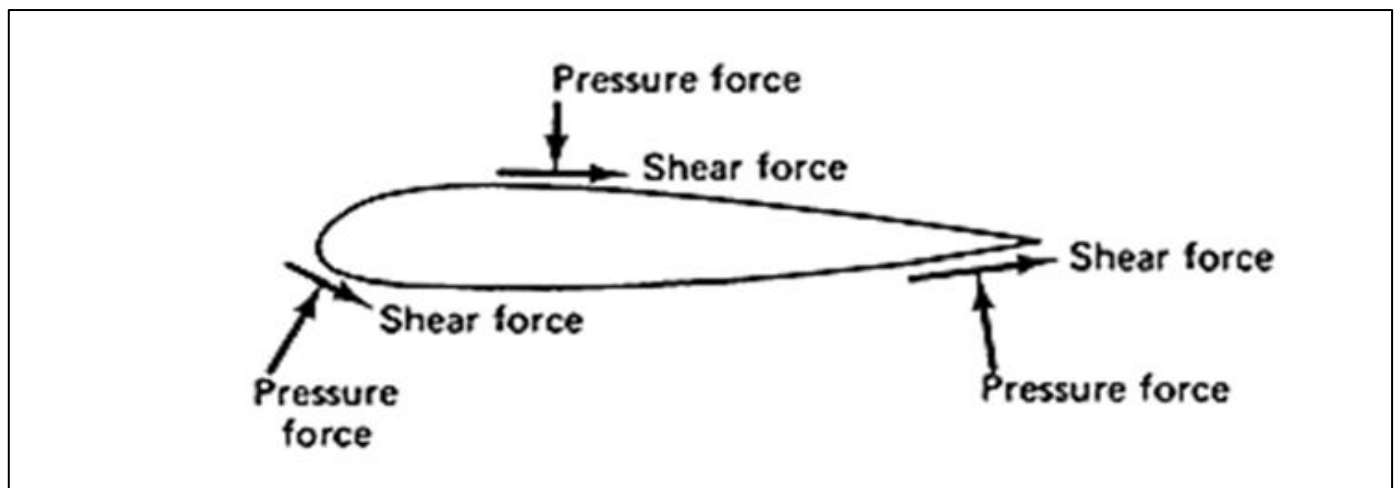


Fig 5: Pressure Forces Orientation Around Aircraft [15].

Figure 5 reveals that the forces effecting on an airfoil are divided into shear forces and pressure. Shear forces result from the air's viscosity, whereas pressure forces emerge because of variations in air velocity as it moves over the aircraft. The pressure distribution on an airfoil produces a net resultant force, typically decomposed into elements like drag and lift, which align with the free stream direction, and axial

and normal forces relative to the orientation of airfoil. This resultant force is commonly articulated as a combination of drag, lift, and a moment around a point a quarter of the way along the chord from the airfoil's leading edge [16].

Figure 6 demonstrates the typical pressure distribution over an airfoil, highlighting how the pressures at any point are transformed into non-dimensional pressure coefficients. This

standardization lets for a clearer comparison and analysis of aerodynamic performance across airfoil shapes and various conditions [17].

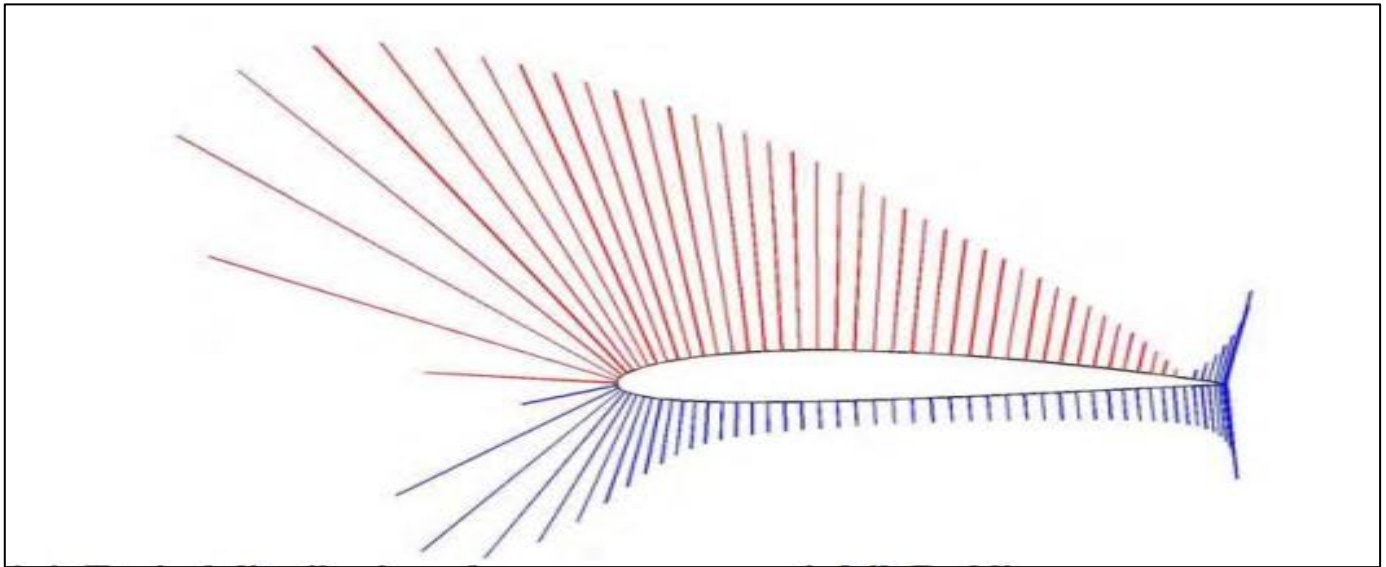


Fig 6: Pressure Distribution Around Airfoil Shapes

C. Aerodynamic Drag

Aerodynamic drag happens when fluid flows around an object, or an object moves over a fluid, exerting force on the object. This force, known as drag, acts opposite to the relative motion between the fluid and the object, producing resistance to the object's movement. For instance, an aircraft or airfoil wing moving through air experiences increasing aerodynamic drag as airspeed increases, given a constant angle of attack. The total aerodynamic drag comprises several elements [18]:

- Induced Drag: Produced by turbulence and vortices from airflow turning and lift-associated downwash. It rises with the angle of attack and decreases as airspeed squares.
- Form Drag (Pressure Drag): Influenced by the airfoil's shape and size, this drag rises with the square of the airspeed. Streamlined designs aid mitigate this drag.

- Friction Drag: Outcomes from air friction on the airfoil's surface, escalating with both surface area besides the square of the airspeed.
- Profile Drag (Viscous Drag): A combination of friction and form drag.
- Parasitic Drag (Interference Drag): Arises from non-lifting aircraft parts like landing gear and fuselage, increasing significantly with airspeed then becoming more prominent at higher speeds.
- Wave Drag: Occurs at supersonic and transonic speeds due to shock waves, notably when crossing the sound barrier, causing a sharp rise in drag.

Each type of drag plays a role in the performance pf aircraft, influencing design considerations to enhance aerodynamic efficiency, especially at operational conditions and varying speeds. Figure 7 illustrates various drag force components:

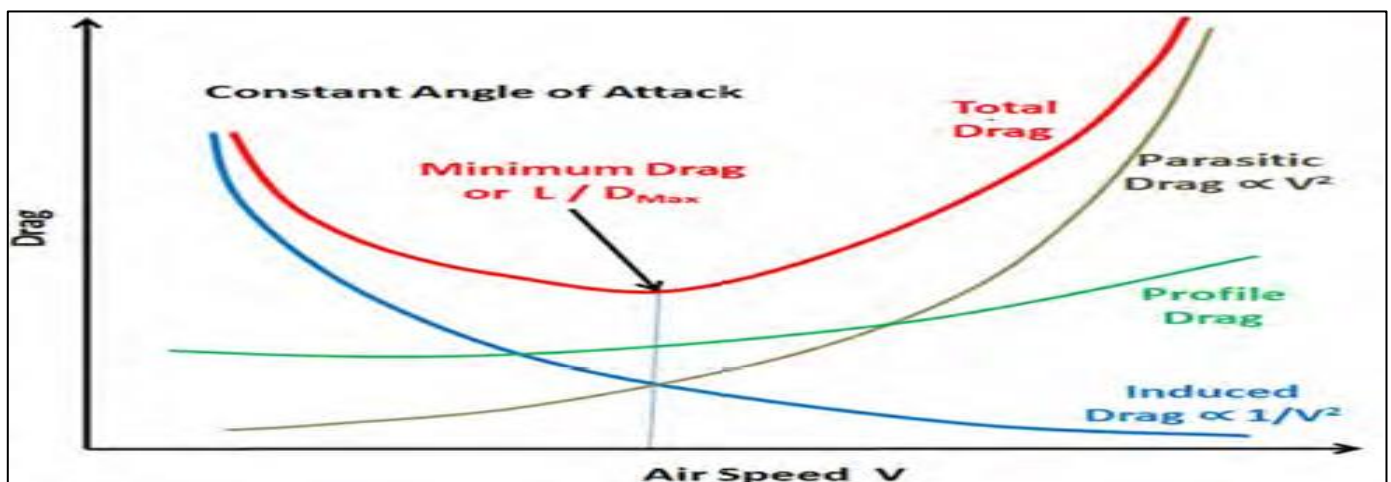


Fig 7: Drag Components [15].

Frequently, drag forces are considered undesirable as they significantly impact overall performance and the fuel consumption of air vehicles. Therefore, engineers invest considerable effort into minimizing these forces to improve the operational capabilities and efficiency of aircraft [18].

D. Drag Coefficient (C_D)

The drag coefficient, often referred to as fluid dynamic drag, computes the resistance an object faces when moving throughout a fluid. However, it is a non-dimensional value, enabling aerodynamicists to consider the shape effects, inclination, and flow conditions on aerodynamic drag. The formula for the drag coefficient is expressed as following [19]:

$$C_D = D / (0.5 \rho v^2 c) \quad \text{Eq.1}$$

Where D signifies the drag force, ρ is the air density, v is the fluid velocity, and c is a characteristic length, typically the chord length of an airfoil or the sphere diameter. This equation allows for accurate adjustments based on varying aerodynamic situations, facilitating the optimization of designs to diminish drag.

E. Aerodynamic Lift

Lift is an aerodynamic force important for keeping an airplane aloft, countering its weight. Primarily produced by the wings, lift results from the aircraft's motion via the air. It is a vector quantity, representing it has both direction and magnitude, and acts perpendicularly to the airflow through the pressure center. However, lift is influenced by the air interaction with the airfoil, counting factors like the airfoil's shape besides the fluid dynamics involved. As air flows around the airfoil, it produces wall shear stresses tangential forces because of friction from the fluid's viscosity in addition pressure stresses, which act perpendicularly because of the pressure distribution around the airfoil [20].

Whereas both stresses contribute to the forces experienced by the airfoil, pressure stresses are mainly responsible for lift. Shear stresses contribute mainly to drag and have a minimal effect on lift. Hence, for streamlined bodies for instance airfoils, it's the pressure distribution around them that predominantly produces lift. Integrating these pressure stresses over the airfoil's surface offers the total lift force, showcasing the critical role of aerodynamic design in flight dynamics.

F. Lift Coefficient (C_L)

The lift coefficient, denoted as C_L , quantifies the lift produced by an aerofoil or wing relative to the angle of attack. This coefficient reveals how the tendency, the shape and given situations of flow affect lift and combines in a single value many interaction of the aerodynamic processes. The equation below for the lift coefficient represents as following [19]:

$$C_L = L / (0.5 \rho v^2 c) \quad \text{Eq.2}$$

Where L stands for the lift force, ρ being the air density, c for the characteristic length, and v for the velocity which can be deemed as airfoil chord.

G. Theory on Flow Separation

In flow separation there is an unsteady boundary layer of a fluid moving via a surface resulting to be unstable. Flow situations. Such pets lead to a rise in pressure drag – a type of drag that happens as a result of changes a load acting perpendicular to a surface and in a direction towards the inside of an object. It is significant to note that separation of flow generally cause wake, in which there exists a recirculation zone that flow is occurring behind the body which rise the level of drag then influences the flow efficacy of an object. Figure 8 signifies boundary layer detachment from a cylinder [15]:

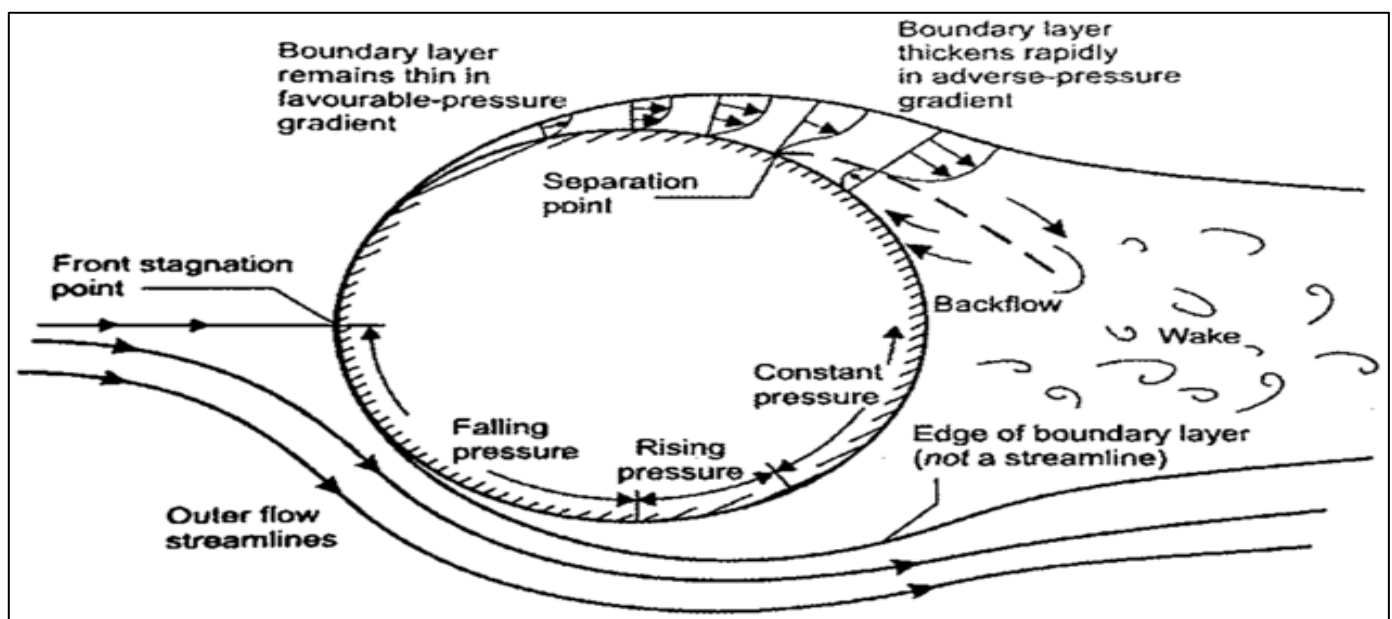


Fig 8: Boundary Layer Detachment from a Cylinder and Directions of Air Flow.

Flow separation produces a turbulence region that significantly increases drag force. To decrease this drag, minimizing flow separation is crucial. Furthermore, flow separation can cause vortex shedding, causing unwanted instability and vibrations. As illustrated in Figure 8, as fluid flows over a sphere, it initially accelerates, generating a favorable pressure gradient where pressure declines along the

flow direction. Nevertheless, beyond a certain point, the flow decelerates, leading to an increase in pressure known as the adverse pressure gradient. This adverse pressure gradient significantly influences the flow dynamics near the surface, possibly exacerbating flow separation problems [21]. Figure 9 illustrates the boundary layer detachment occurring on the upper surface of a wing:

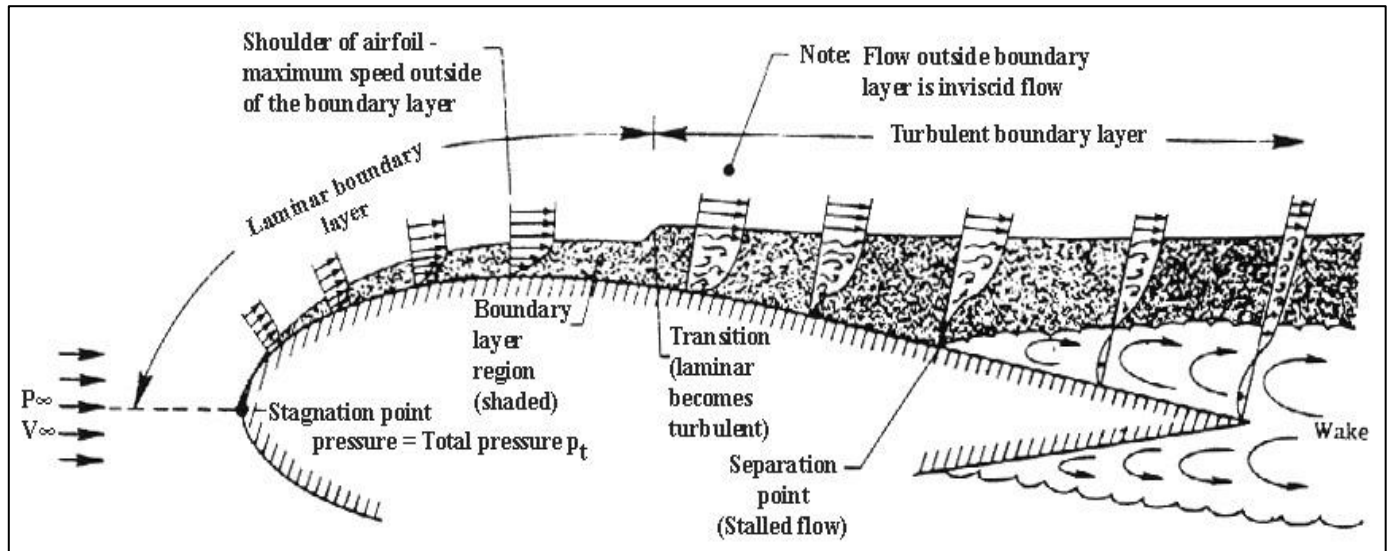


Fig 9: Boundary Layer Detachment Occurring on the Upper Surface of a Wing [21] .

When a significant increase in pressure happens, the flow may oppose direction. Since it cannot travel backward because of the incoming fluid, it detaches from the surface, causing flow separation. For instance, as depicted in Figure 9, flow separation around a flat sphere in laminar flow happens at approximately 80 degrees. Though, if the boundary layer is turbulent rather than laminar, it better follows to the surface, delaying flow separation to around 120 degrees and significantly dipping pressure drag. This delay is because of turbulence enhancing the mixing of various flow layers, facilitating momentum transfer, and letting the flow to withstand larger opposing pressure gradients deprived of separating [22].

H. NACA 0012 Airfoil Use

NACA 0012 is a symmetric airfoil intended by the National Advisory Committee for Aeronautics (NACA), a precursor to NASA. This airfoil has been widely studied and used because of its stable and predictable aerodynamic performance under different flight conditions. As a symmetric airfoil, the NACA 0012 does not have camber, which means it produces no lift at zero angle of attack, making it ideal for experimental analysis and scientific research where controlled situations are paramount [23].

The versatility and simplicity of the NACA 0012 airfoil make it mainly useful in applications needing accurate control over aerodynamic forces, for instance in testing environments and wind tunnels. Its design characteristics permit for a balanced trade-off between drag and lift, offering a baseline model for evaluating advancements and modifications in airfoil technology [24].

III. METHODOLOGY

A. Model Material and Geometry

The NACA 0012 design was brought into ANSYS 2023 through spaceclaim. A fluid domain corresponding to the profile was made after the shape was made. After that, the domain of fluids was brought into ANSYS Fluent so that CFD models could be simulated. Around the aerofoil blade, a fluid region was made. The aerofoil was contained within a single flowing domain. This was carried out to improve the quality of the mesh near important areas. Figure 10 shows the imparted blade geometry and Figure 11 show the fluid enclosure surrounded the blade with 3750 mm for each side of the cube:

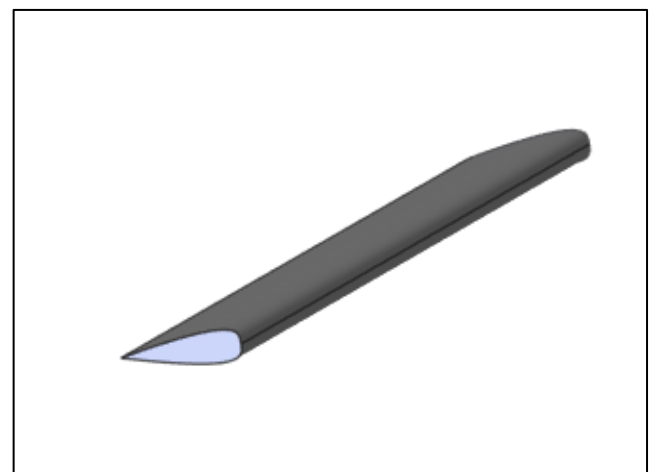


Fig 10: The Fluid Enclosure Surrounded the Blade

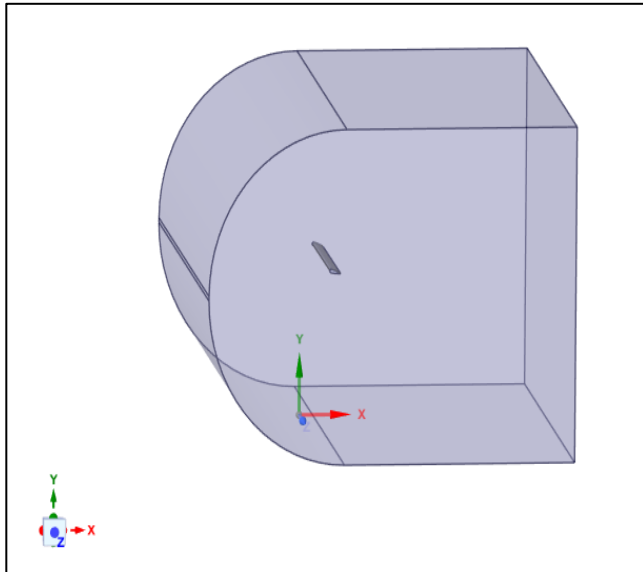


Fig 11: Imparted Blade Geometry

B. Computational Fluid Dynamics Modelling

After finalizing the geometry, the ANSYS workbench was run and geometry was imported in Fluent.

• Meshing

After giving the airfoil and the sides of the domain names, they were chosen, in addition mesh controls have been placed on them. The bottom, the top, the inlet, the exit, and the airfoil are all given body sizing. Meanwhile, inflation It was assigned to the bottom and the wing as limits. With Ansys Mechanical, a model of mesh was created. During mesh creation, inflation, body sizing, and method were some of the adjustments that were made to the mesh. The mesh size close to the aerofoil edges was given extra care.

The method of Multizone mesh was selected as well for the whole model since it's automatically splits the geometry model into mapped either structured or sweepable parts and free (unstructured) areas. When possible, a pure tetra/pyramid mesh will be generated. In places that are harder to catch, it uses an unstructured mesh to fill in the gaps. If the method of Multizone mesh is determined, all areas are mapped with a clean hexahedral mesh if it is possible to do so. Figure 12 shows a capture screen of Multizone method details:

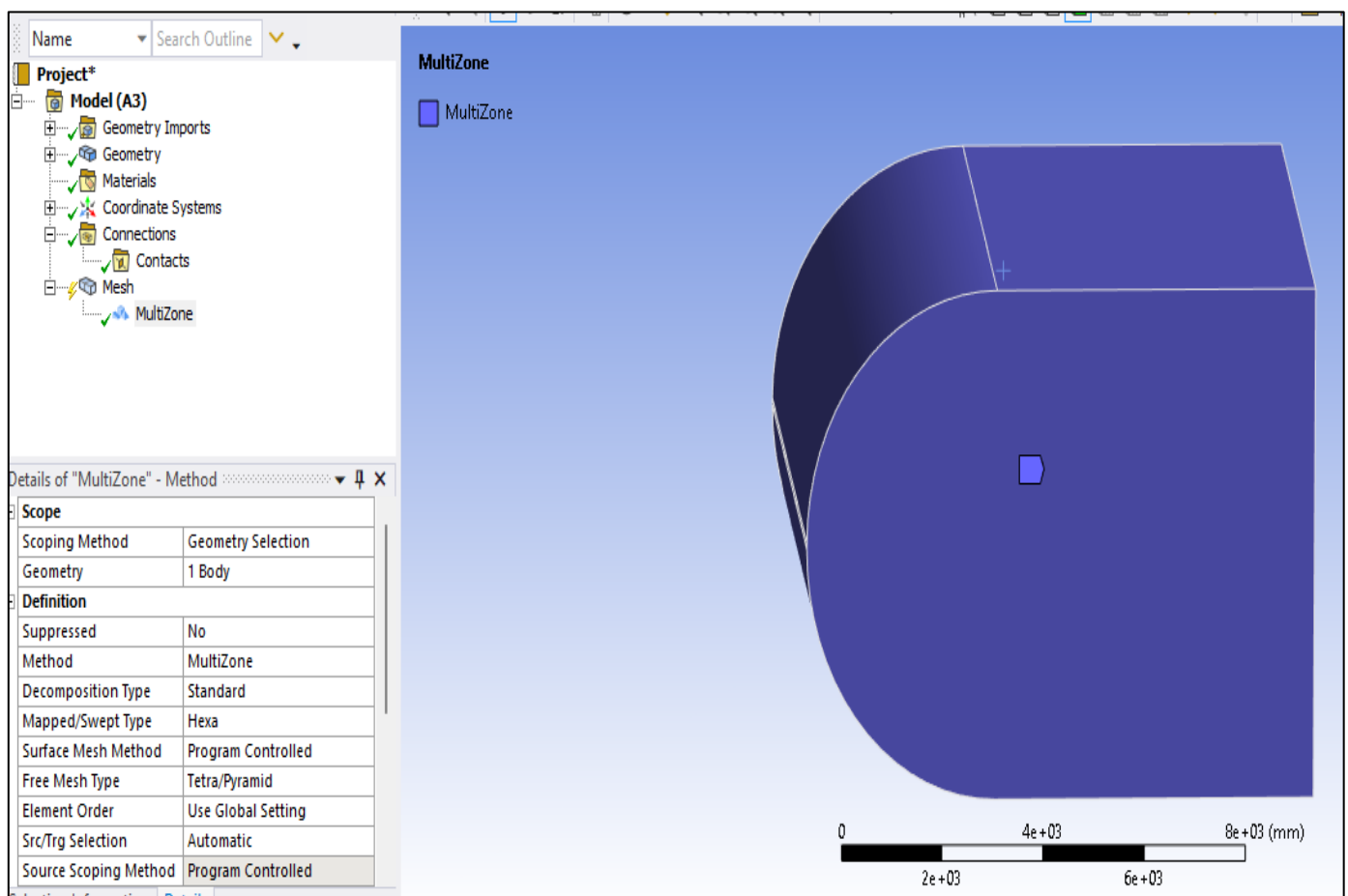


Fig 12: Details of Multizone Method

The final mesh that was made for this study is shown in Figure 13. CL and CD were the factors that were observed for convergence.

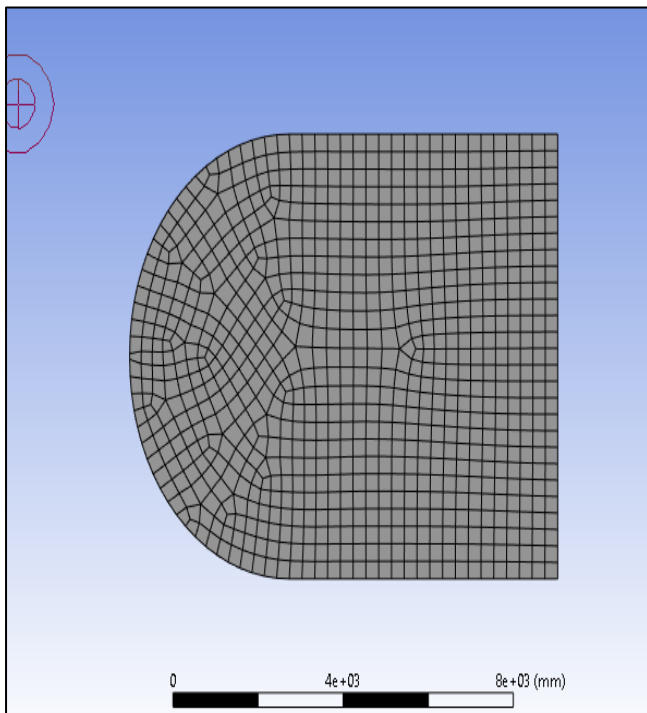


Fig 13: The Final Modelled Mesh.

When you do a CFD analysis, named selection represents one of the most essential processes because it makes setting the boundary conditions easy. Figure 14 shows the named choices that were used in this study. They are inlet, outlet, right, left, top, bottom, and wing surface:

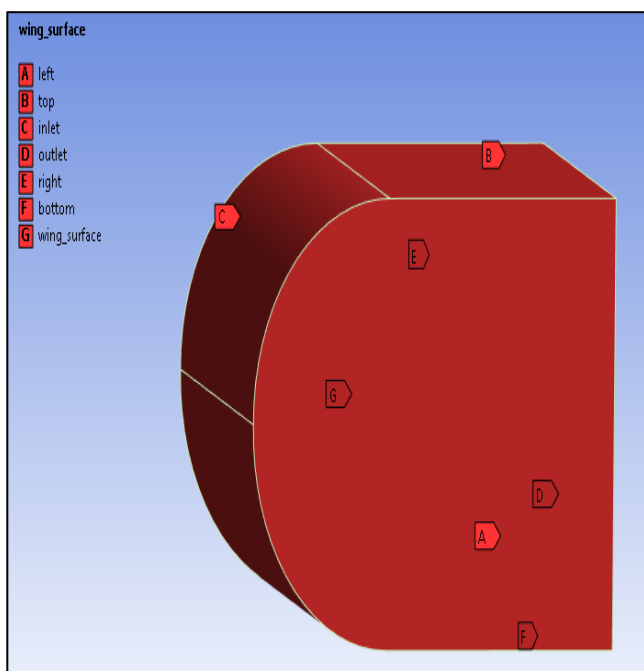


Fig 14: The Named Choices Used

Mechanical Analysis has been closed while fluent is run after named pick and meshing. Since we need to look at various AOA in this case, both the vertical and horizontal parts of the speed need to be found at each AOA. It is chosen that the solver be double precision and that the type of solution be pressure based. The turbulence model of K- ω SST has been chosen for this research. A well-known eddy-viscosity model is the turbulence model of SST k- ω , which is made up of two equations. The SST method takes the best parts of two different approaches and puts them together in one. The SST k- ω model is capable of being used as a Low-Re turbulence model without any extra damper functions because it uses the formulation of k- ω in the inner regions of the layer that forms the boundary.

Figure 15 shows the graphics of the model in the CFD fluent indicating the velocity inlet within the blue zones and arrows and the pressure outlet within the red cone and arrows:

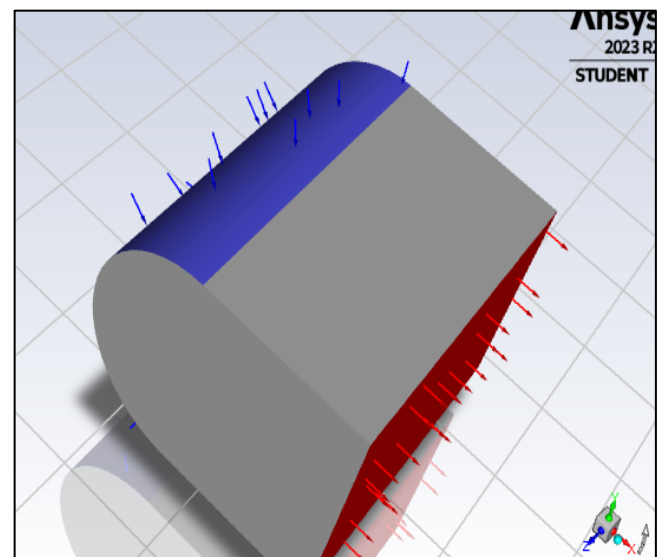


Fig 15: The graphics of the model in the CFD fluent.

Figure 16 shows the setting of the inlet zone in the CFD, where the velocity was set at 50 m/s and the pressure at 99745 Pa with a temperature of 309.6 K:

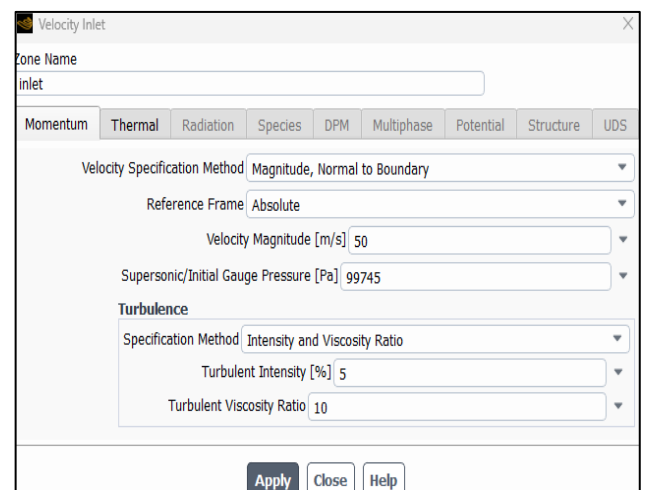


Fig 16: The Setting of the Inlet Zone in the CFD.

Figure 17 shows the setting of the outlet zone in the CFD, where the pressure at 99745 Pa with a temperature of 309.6 K:

Fig 17: The Setting of the Outlet Zone in the CFD.

Figure 18 shows the reference values setting based on the projection report computation of the wing surface at 0 degree of attack angle:

Fig 18: The Reference Values Setting

Different cases, with fixed components of inlet velocities (50 m/s), were generated to study the effect of changing the angle of attack varying from 0-25 with a step of 5 degrees.

IV. RESULTS AND DISCUSSION

This chapter shows the lift and drag coefficients that change with the number of iterations, along with the pressure and streamline velocity contours that come from CFD simulations for different angles of attack for the NACA0012 airfoil's wing surface. The angles of attack range from 0 to 25 degrees. The selected airfoil is NACA0012 which is a symmetrical airfoil. Because of this, the angle of attack is the only thing that will cause lift. It fails to produce any lift at a 0° angle of attack, which will be presented and shown in the ANSYS fluent outcomes after the CFD computations. At an angle of attack of 0 degrees, a suction action can be seen on the lower surface. This happens because of a convergent-divergent passage forming within the airfoil along with the ground. The flow velocity rises among the ground's surface and the lower surface, which lowers the pressure and lowers the lift force in that area. This chapter is divided into main subsections: the outcomes of the CFD computations in terms of the lift and drags coefficients with respects to the number of iterations as well as the contours of pressure magnitude and streamline velocity and the performance of the airfoil under varying AoA.

A. CFD Results: Lift and Drag Coefficient and Pressure and Velocity Contours

This subsection presents the CL and CD in terms of the number of iterations number of 100 iterations as assigned in the run calculation settings as well as the pressure and velocity contours under varying AoA:

• 0° Angle of Attack

Figure 19 shows the CL in terms of 100 iterations concerning the wing surface when the AoA was adjusted at 0 degree:

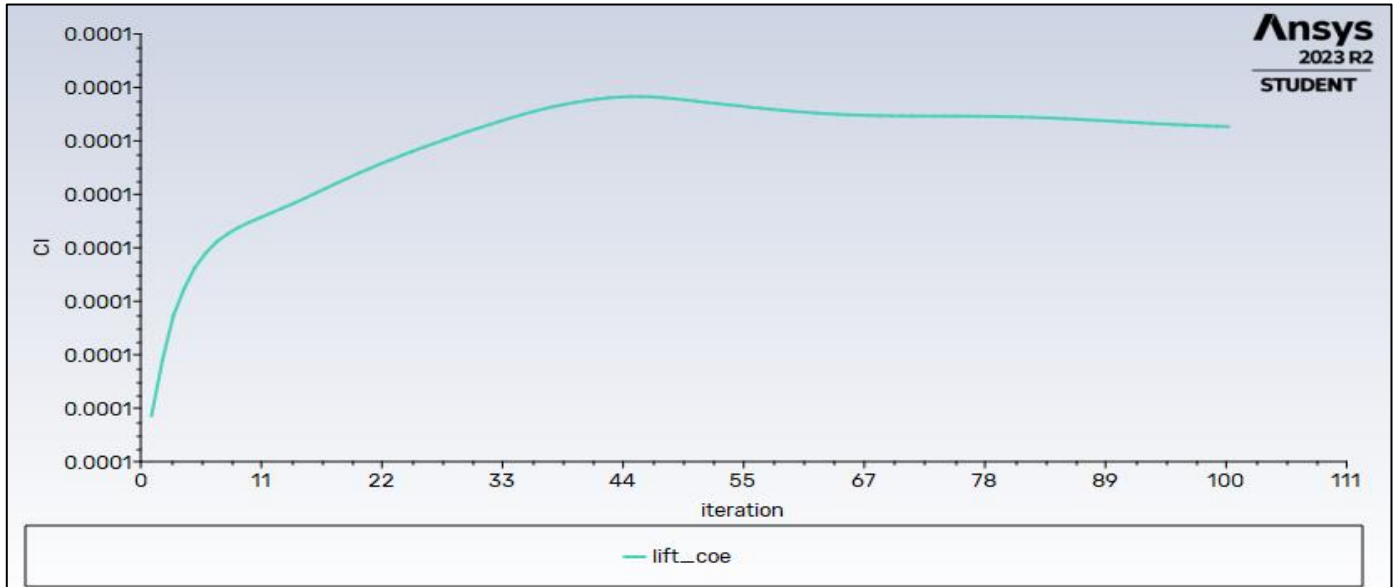


Fig 19: Lift coefficient values under 0-degree AoA.

After 93 rounds of iterations, the coefficient of lift has reached a settled value. When there is no angle of attack, the lift coefficient is 0.0001 as shown above. It is not responsible for any lift when looked at a 0 AoA. At an angle of attack of 00 degrees, a suction action can be seen on the lower surface. This happens because of a convergent-divergent passage

forming between the airfoil and the ground. The flow speed rises between the ground and the lower surface, which lowers the pressure and lowers the lift force in that area. Figure 20 shows the CD in terms of 100 iterations concerning the wing surface when the AoA was adjusted at 0 degree:

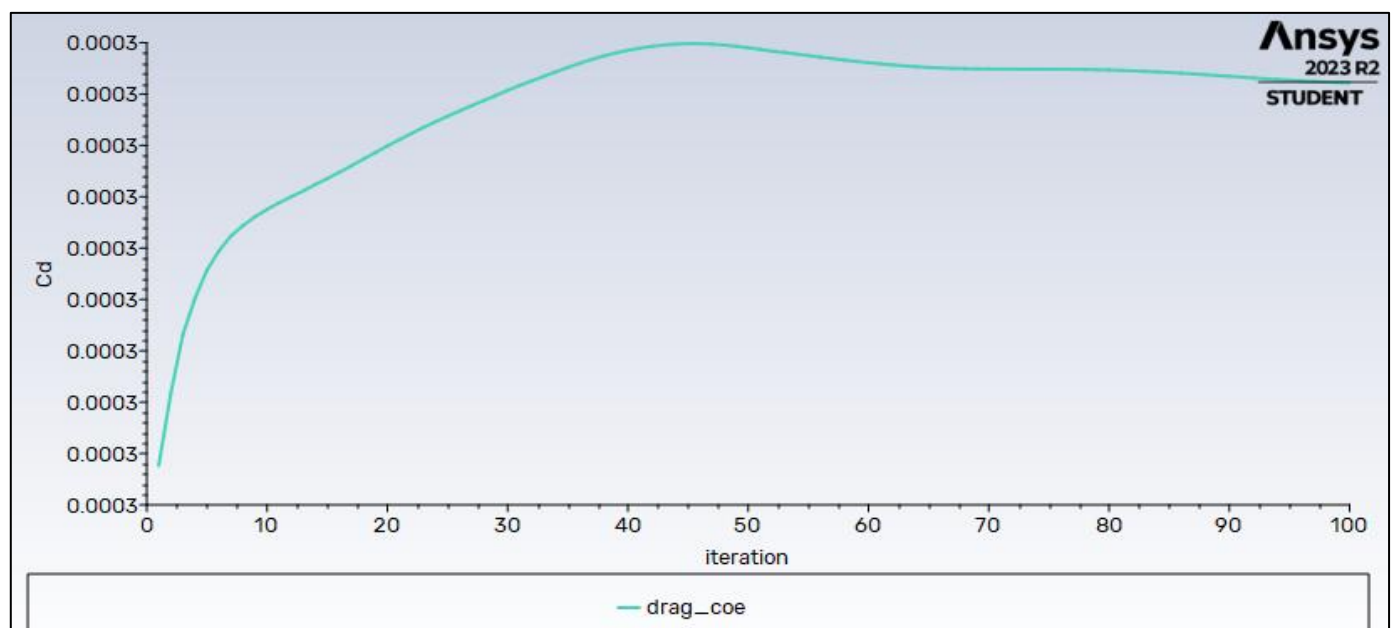


Fig 20: Drag Coefficient Values Under 0-Degree AoA.

Based on the above drag plot, the drag coefficient is 0.0003 at the same number of iterations (93). Figure 21 shows

the pressure magnitude in terms of contours concerning the wing surface when the AoA was adjusted at 5 degree:

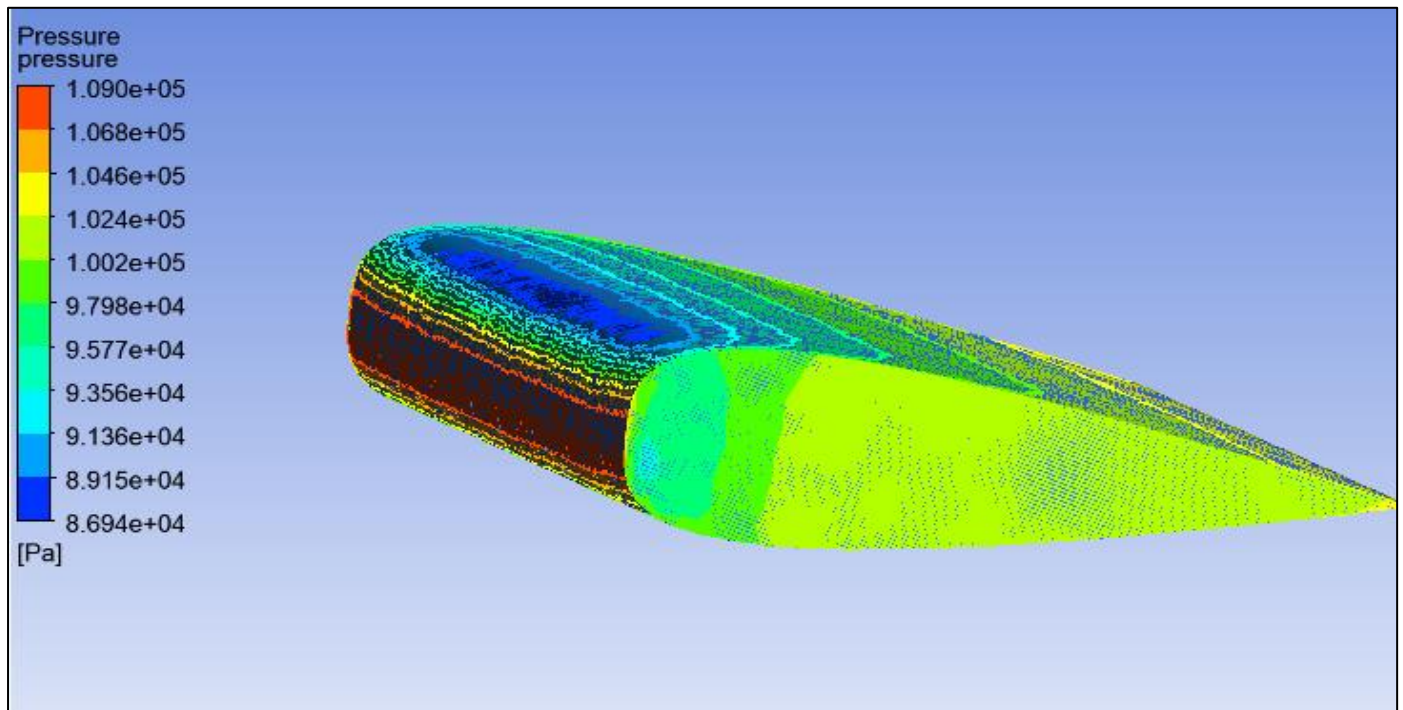


Fig 21: Pressure Contour Under 0-Degree AoA.

Pressure at 0° is, 1.09×10^5 Pa. The pressure changes are sensitive and allow to infer that the broad picture of (static) air resistance across both face and bottom doesn't change much as it being tilted, which likely bespeaks an

overall steadiness in mid flow around this shape. Figure 22 shows the streamline velocity magnitude in terms of contours concerning the wing surface when the AoA was adjusted at 0 degree:

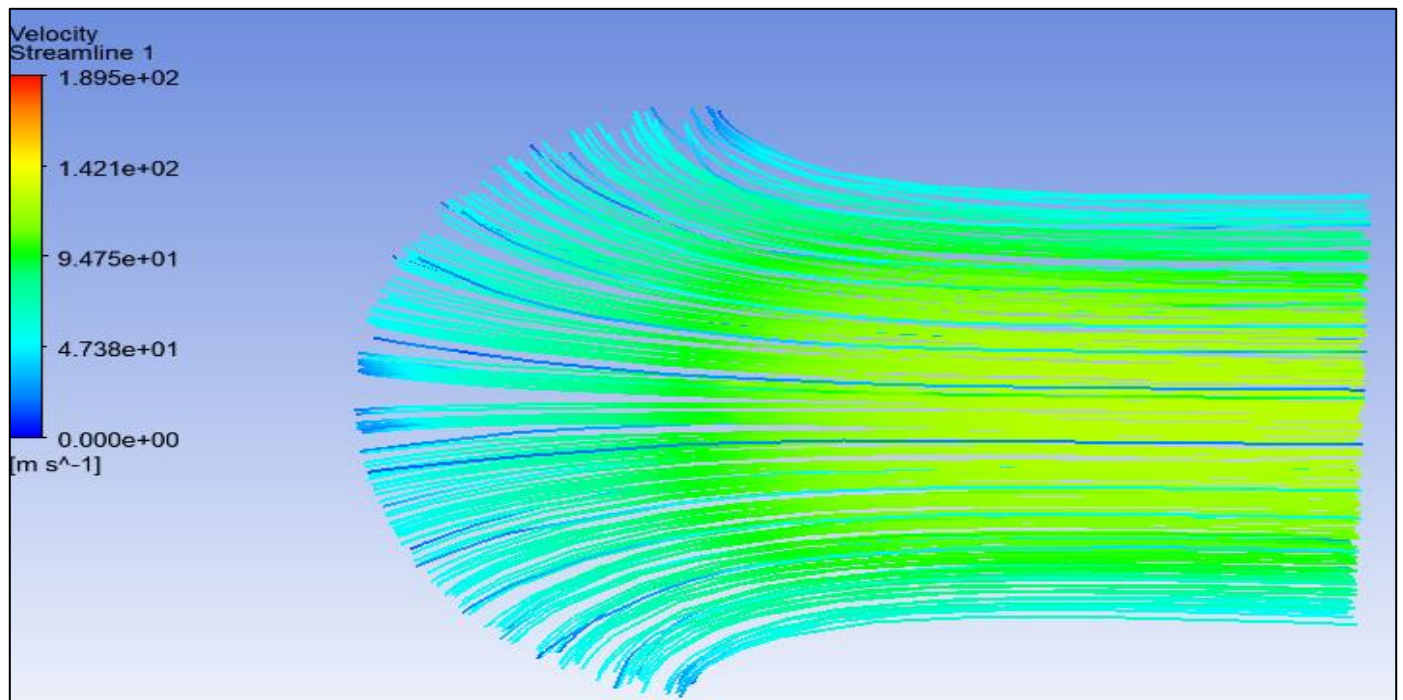


Fig 22: Streamline velocity contour under 0-degree AoA.

From the contour shown above, it can be seen that when airfoil goes through a flow of air, the speed will streamline velocity will rise and show up on the top of the airfoil. Also, it will be easy to see the air separation when the angle of attack goes up after the stalling point.

- *5° Angle of Attack*

Figure 23 shows the CL in terms of 100 iterations concerning the wing surface when the AoA was adjusted at 5 degree:

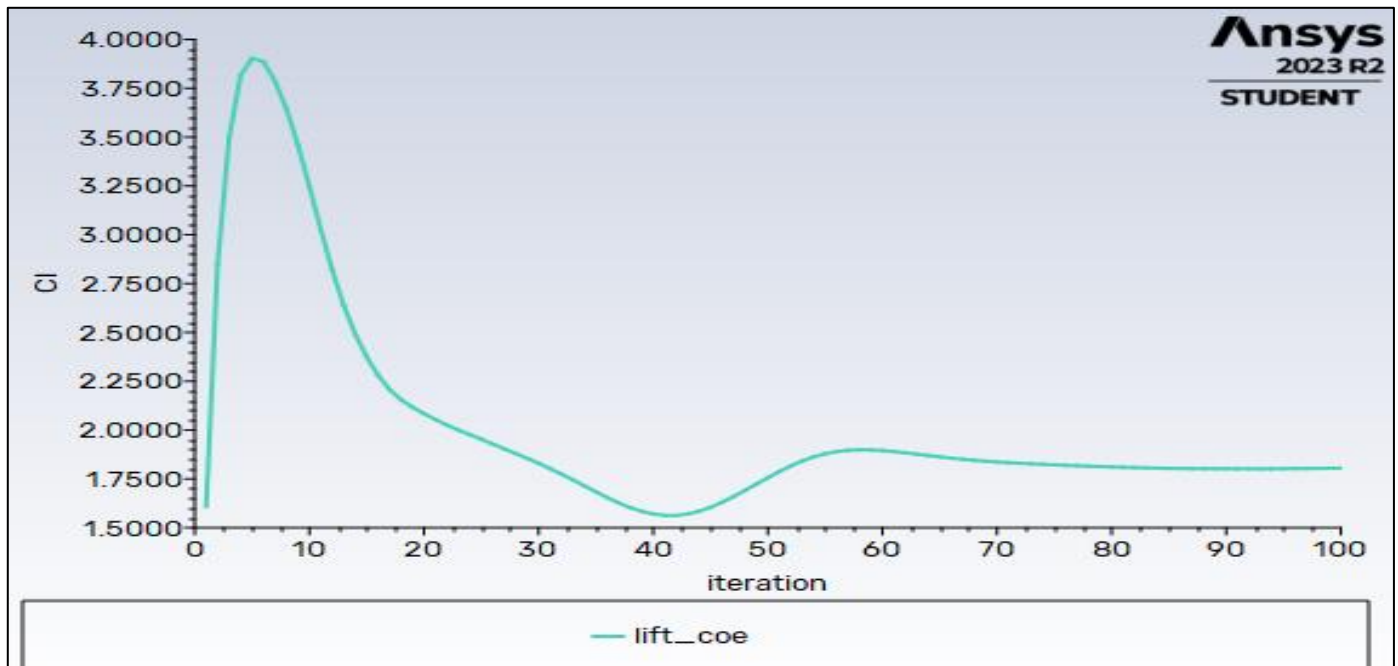


Fig 23: Lift Coefficient Values Under 5-Degree AoA.

After roughly 80 rounds of iterations, the coefficient of lift has reached a settled value. When there is an angle of attack of 5 degrees, the lift coefficient is 1.86 as shown above. The lift coefficient increased from 0.001 to 1.86 at an angle of 0° the aerofoil is set up with a straight airflow, and

produces no lift. Likewise, a small positive increase to 5° translates into an effective angle of attack for generating lift. Figure 24 shows the CD in terms of 100 iterations concerning the wing surface when the AoA was adjusted at 0 degree:

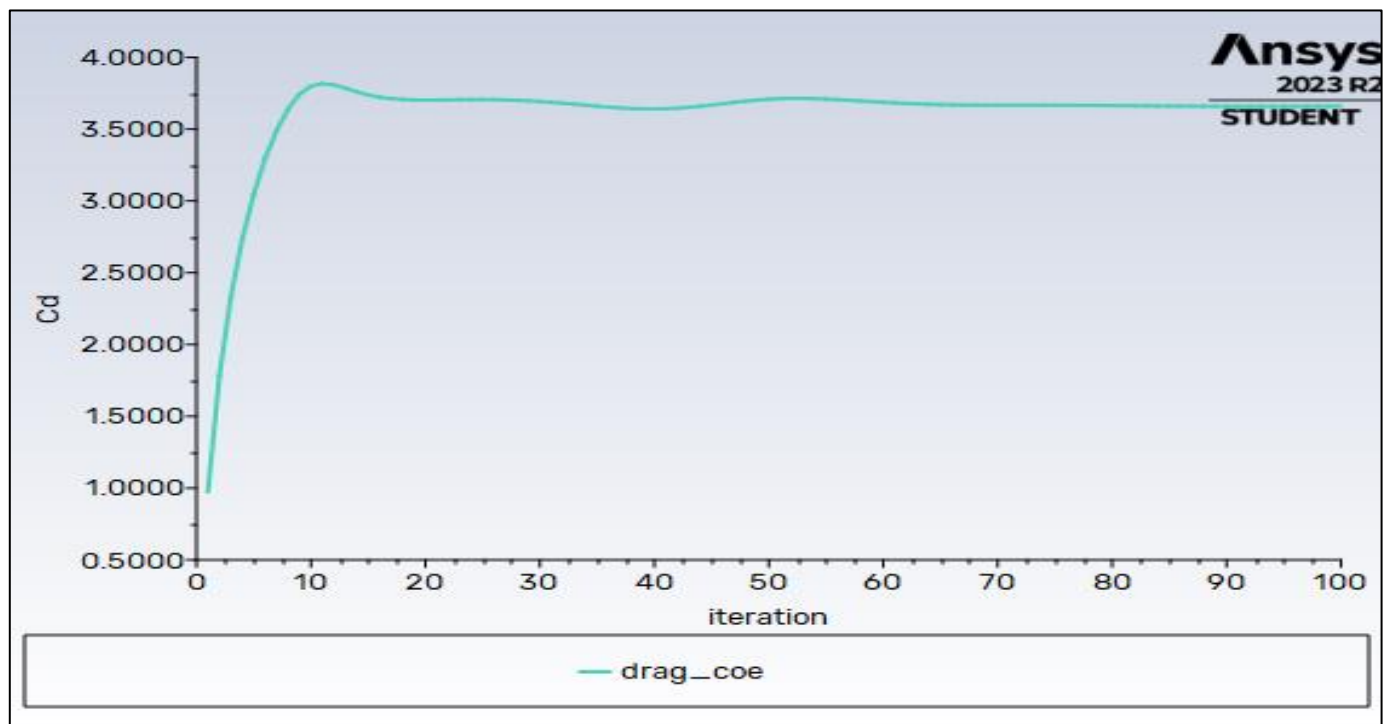


Fig 24: Drag Coefficient Values Under 5-Degree AoA.

Based on the above drag plot, the drag coefficient is 3.75 at the same number of iterations (80). A large increase from 0.0003 to 3.75 is observed, signifying an intense amount of air flow resistance as the aerofoil starts departing further

away from diffusion airflow streamline. Figure 25 shows the pressure magnitude in terms of contours concerning the wing surface when the AoA was adjusted at 5 degree:

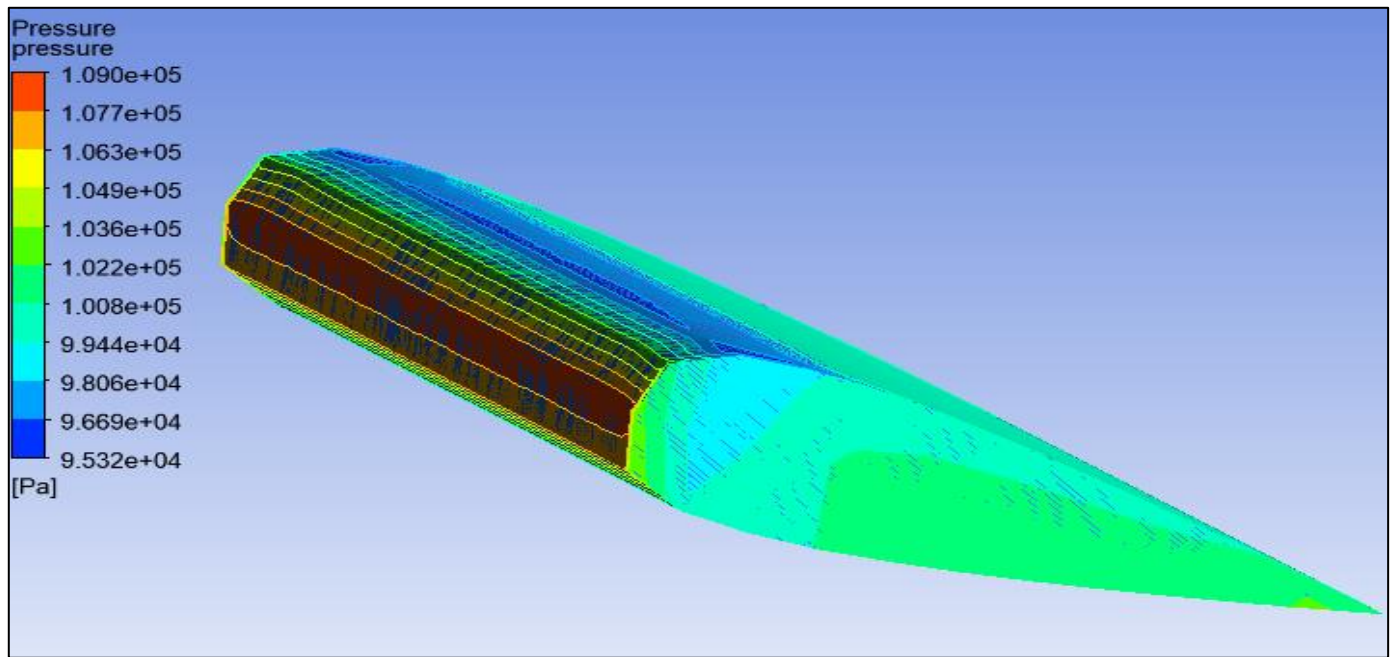


Fig 25: Pressure Contour Under 5-Degree AoA

The pressure contour almost constant around $\approx 1.09 \times 10^5$ Pa after increasing the AoA from 0 to 5-degrees. This stability indicates that the pressure environment is only very mildly influenced by even a small increase in angle.

Figure 26 shows the streamline velocity magnitude in terms of contours concerning the wing surface when the AoA was adjusted at 5 degree:

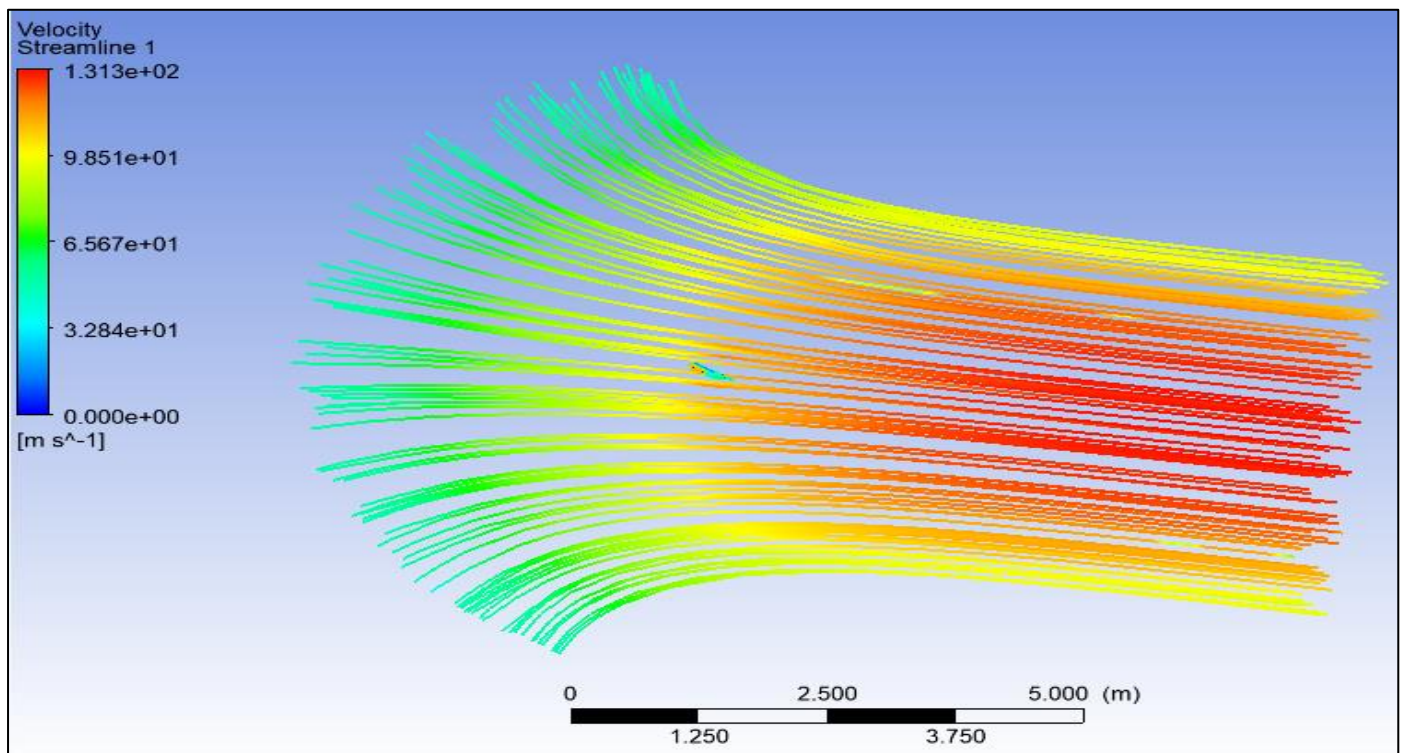


Fig 26: Streamline Velocity Contour Under 5-Degree AoA

After increasing the AoA from 0 to 5-degrees, the streamline velocity decreased from 189.3 down to 131.6 m/s. This decrease in velocity represents the fact that as soon an airfoil starts producing lift, it diverts some of streamline flow path such higher interference.

- *10° Angle of Attack*

Figure 27 shows the CL in terms of 100 iterations concerning the wing surface when the AoA was adjusted at 10 degree:

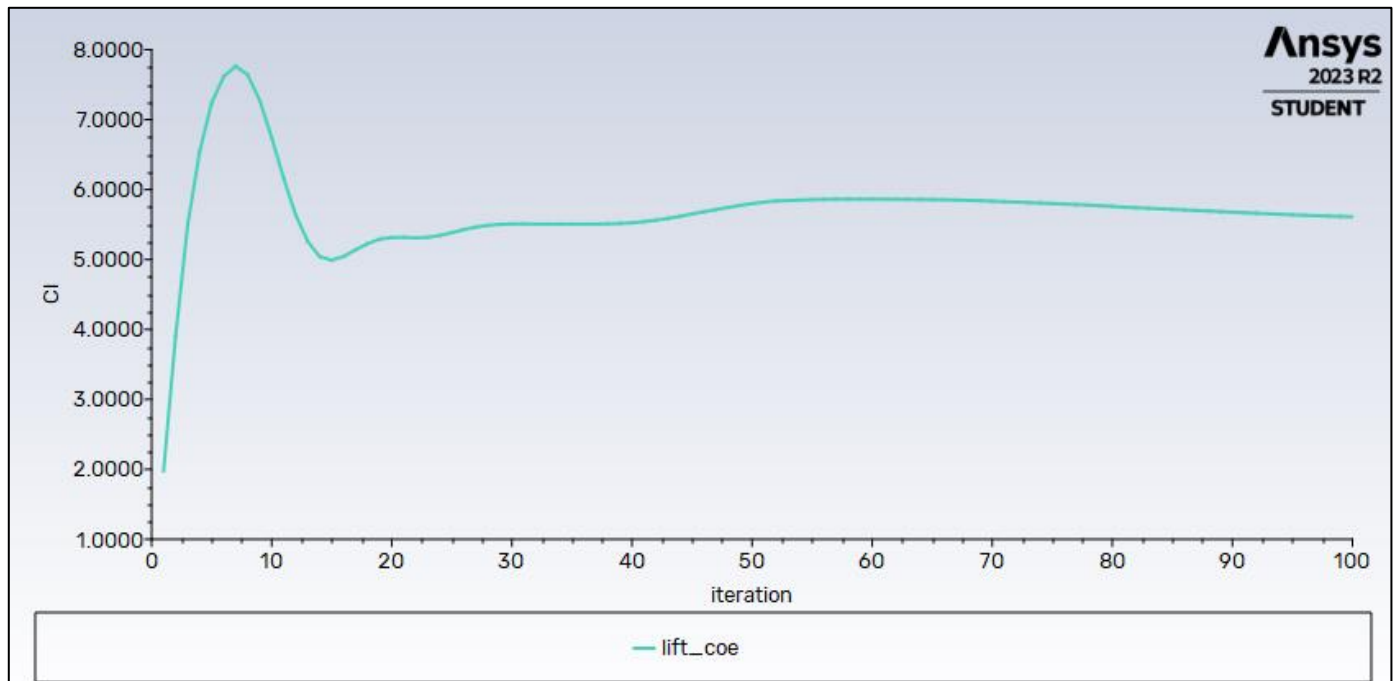


Fig 27: Lift Coefficient Values Under 10-Degree AoA

The lift coefficient has stabilised as a function of iterations at these values for around 60 rounds. As it shown above, lift coefficient is 6 at their angle of attack equal to 10 also when they seek an angle of attack which is ten degrees. CL Continues to grow rapidly from 1.86 so up at 6, this

represents an additional increase in lift as the larger angle allows the airfoil to use more area above and below itself deflecting air downwards. Figure 28 shows the CD in terms of 100 iterations concerning the wing surface when the AoA was adjusted at 10 degree:

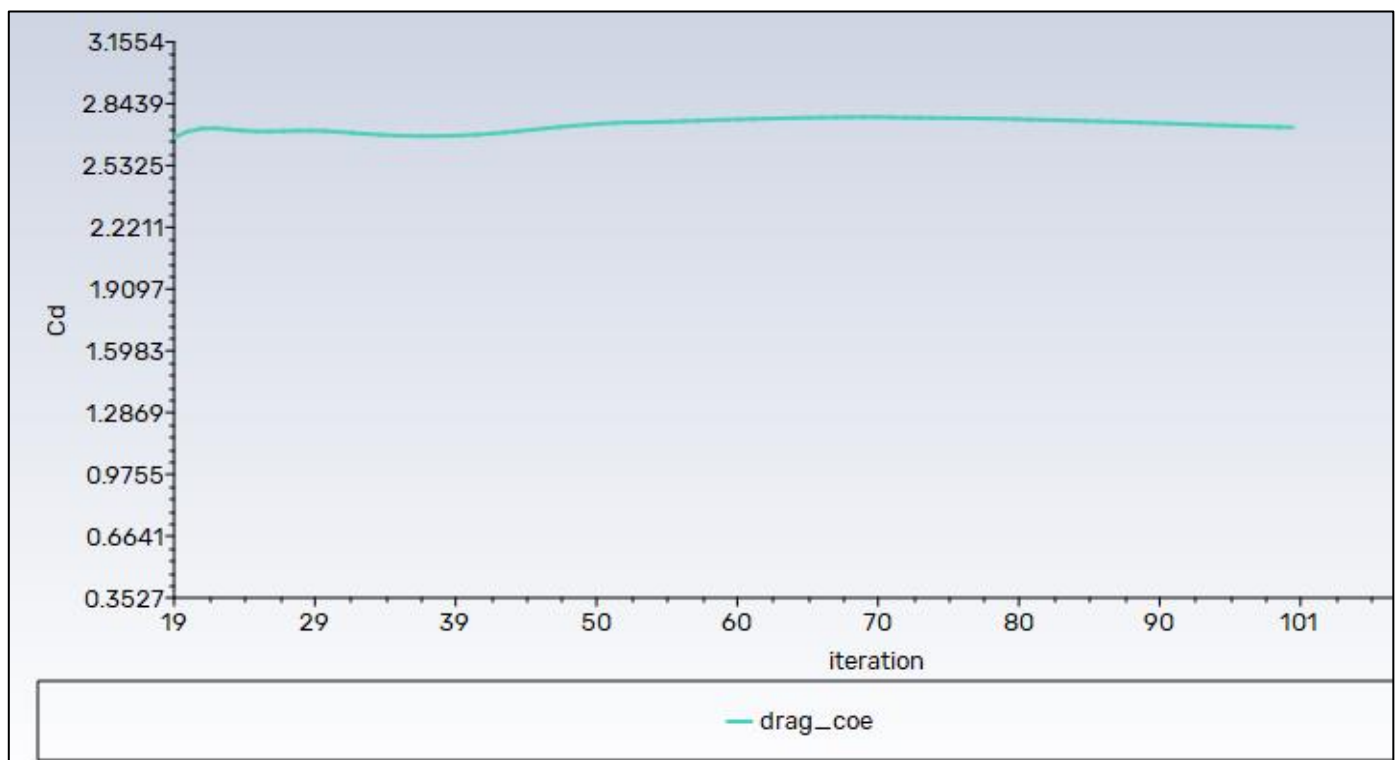


Fig 28: Drag Coefficient Values Under 10-Degree AoA

At iterations of 60 the lift coefficient is incorrect (high) as shown in above drag plot, and hence corresponding to that value of $C_d = 2.63$ with same number of iterations (60). Drops from 3.75 to 2.63, indicating a cleaner interaction despite the

higher angle, possibly due to smoother flow attachment. Figure 29 shows the pressure magnitude in terms of contours concerning the wing surface when the AoA was adjusted at 10 degree:

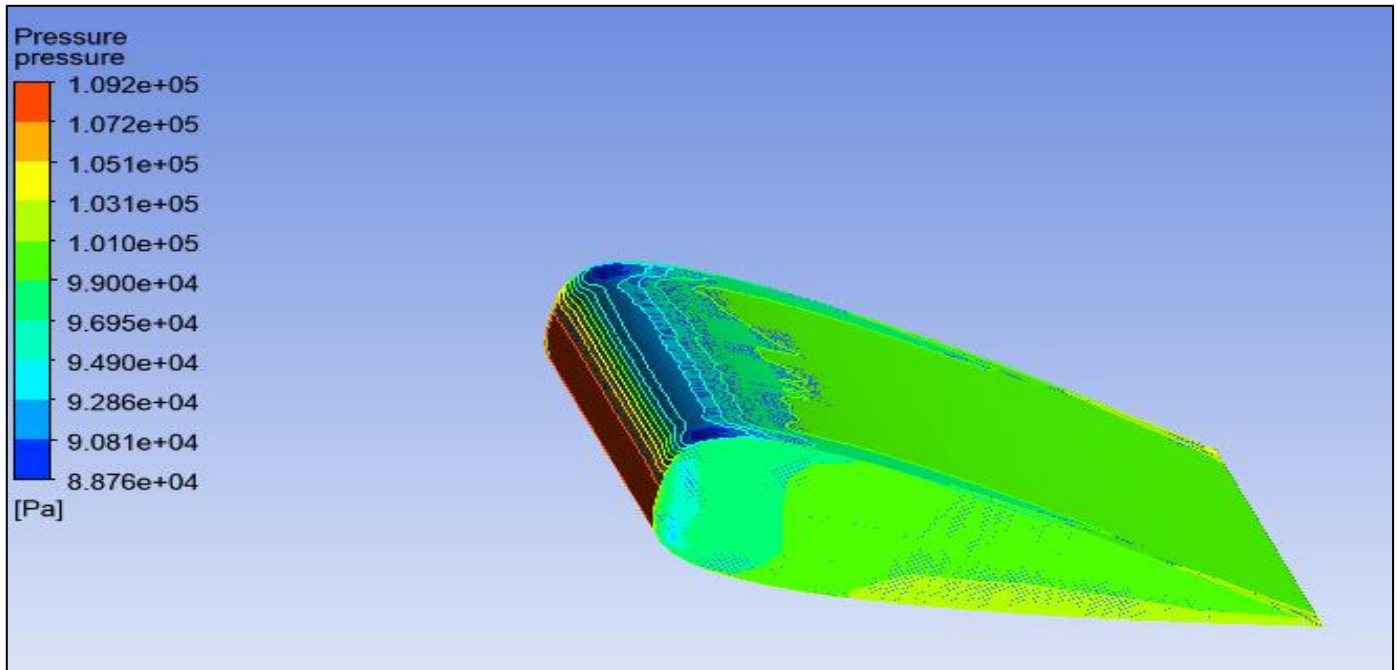


Fig 29: Pressure Contour Under 10-Degree AoA.

When the AoA increases from 5 to 10-degrees, due to increasing in kinetic energy of airflow over wing then so does pressure slightly build-up to $1.092 \times 10^5 \text{ Pa}$. The change in the density and acceleration of airflow over the airfoil areas can

be attributed to this increase. Figure 30 shows the streamline velocity magnitude in terms of contours concerning the wing surface when the AoA was adjusted at 10 degree:

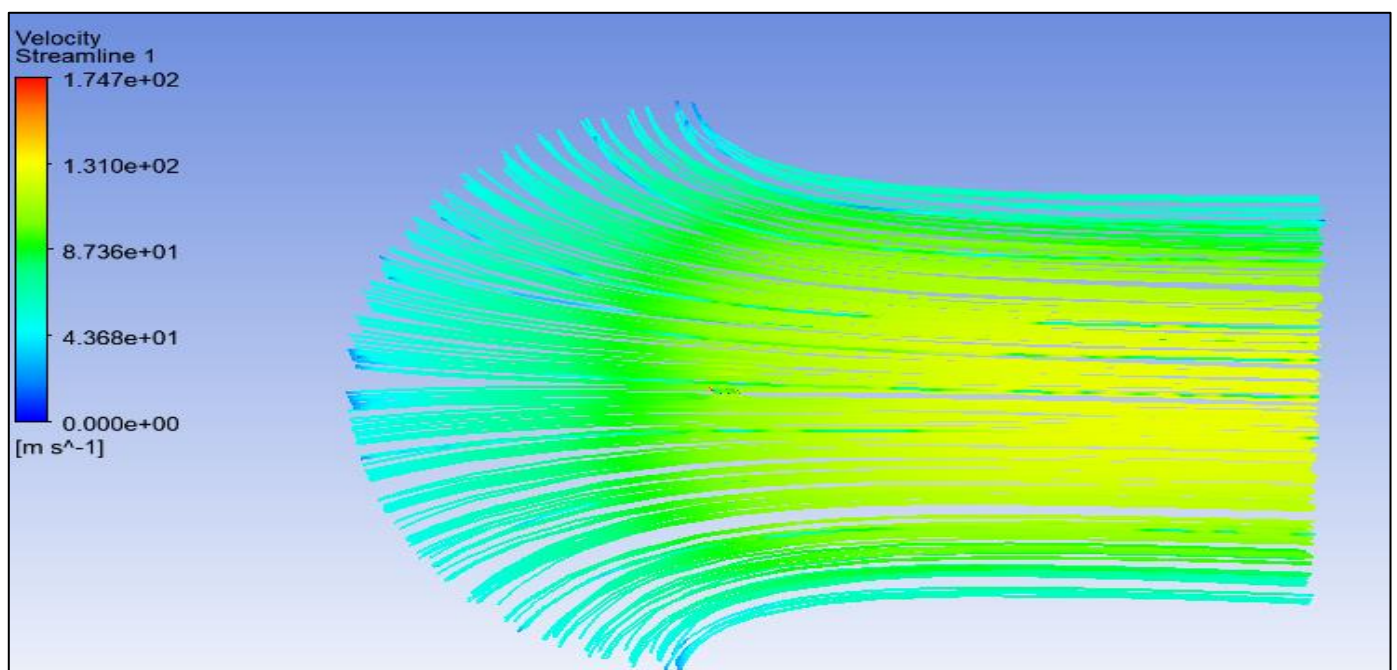


Fig 30: Streamline Velocity Contour Under 10-degree AoA

The streamline velocity then Jumps to 174.7 m/s, indicating a further disturbance in the flow field after increasing the AoA from 5-10 deg; nevertheless, this increase may also imply that even though there is still an unsteady pattern near zero angle of attack (AoA), at higher angles more and more aerodynamic behavior tends towards conforming with traditional flight theory expectations for overall smooth

airflow directed around equally sharp trailing edges suitable for non-shock-producing drag formation.

- *15° Angle of Attack*

Figure 31 shows the CL in terms of 100 iterations concerning the wing surface when the AoA was adjusted at 15 degree:

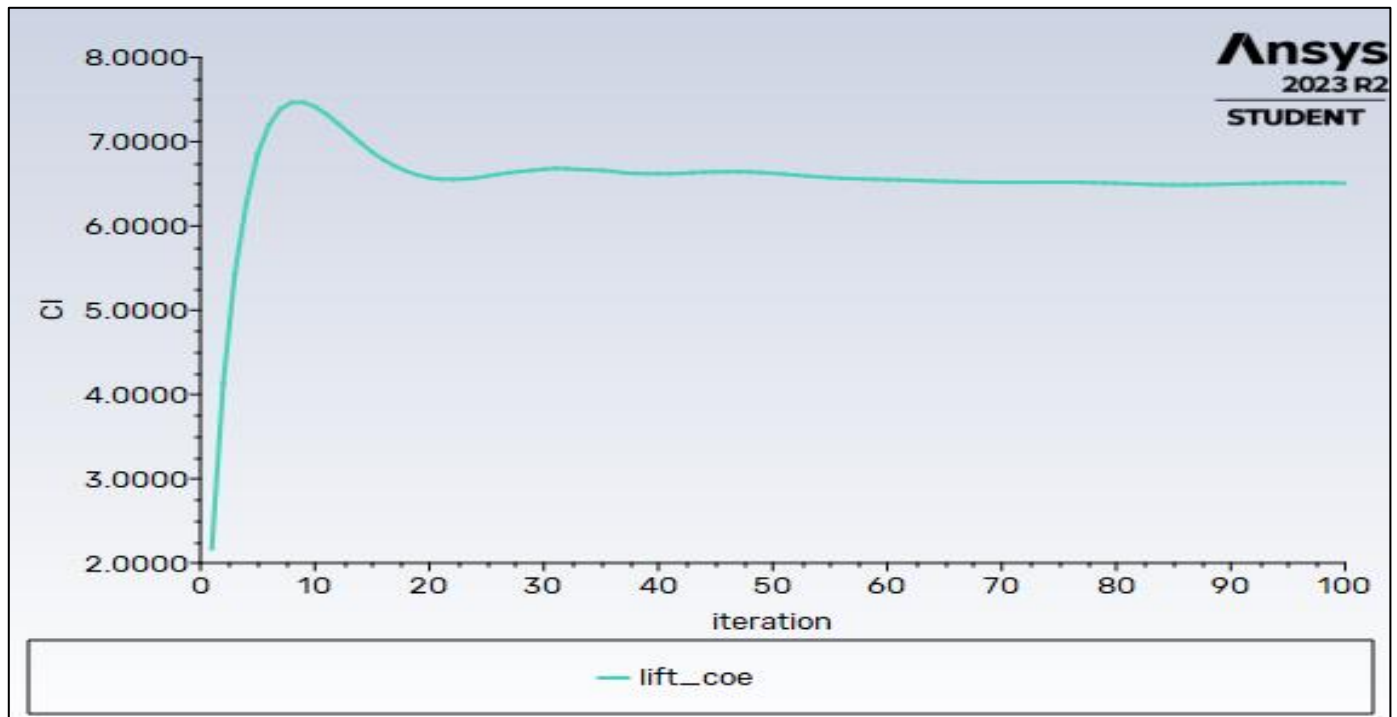


Fig 31: Lift Coefficient Values Under 15-Degree AoA

After around 58 iterations that figure has stabilized at C_L is 6 (An AOA of 15 degrees) – marginally increases from 6 to 6.5, an increasingly diminishing return in lift due to the fact the airfoil is close to the critical angle where flow

separation just begins. Figure 32 shows the C_D in terms of 100 iterations concerning the wing surface when the AoA was adjusted at 15 degree:

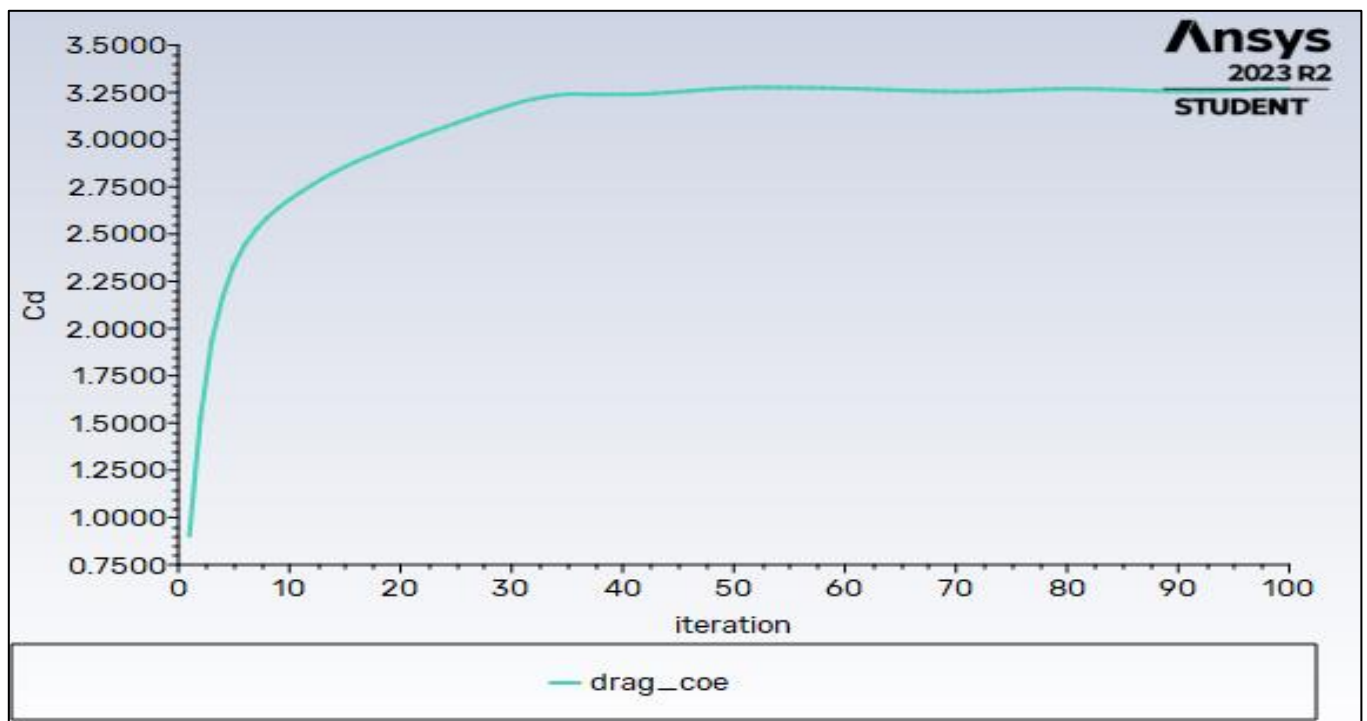


Fig 32: Drag Coefficient Values Under 15-Degree AoA.

The drag coefficient is 3.25 at 58 iterations, the same as above. It increases from 2.63 to 3.25 due to the increased drag resulting from the more severe separation. Figure 33 shows

the pressure magnitude in terms of contours concerning the wing surface when the AoA was adjusted at 15 degree:

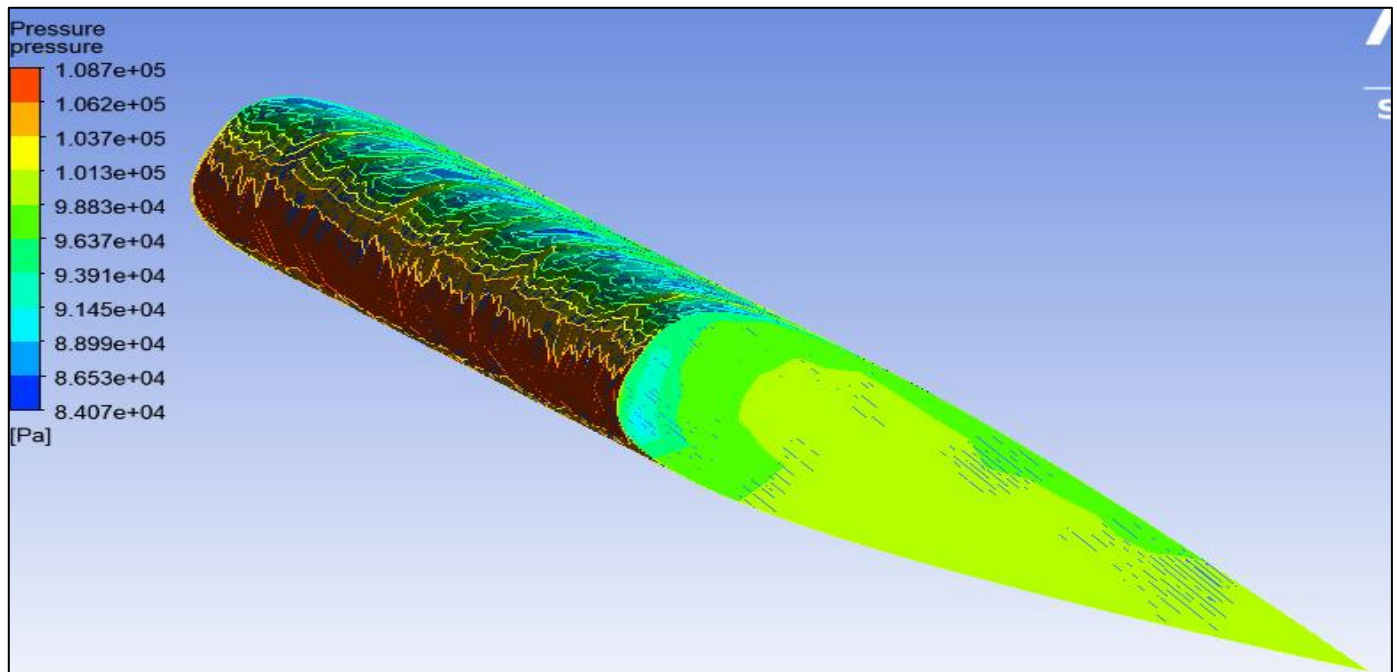


Fig 33: Pressure Contour under 15-degree AoA.

The pressure contour after increasing AoA from 10 to 15-degrees decreased to 1.087×10^5 Pa. This reduction could signify the initiation of largely separated flow, resulting in a

localized pressure loss. Figure 34 shows the streamline velocity magnitude in terms of contours concerning the wing surface when the AoA was adjusted at 15 degree:

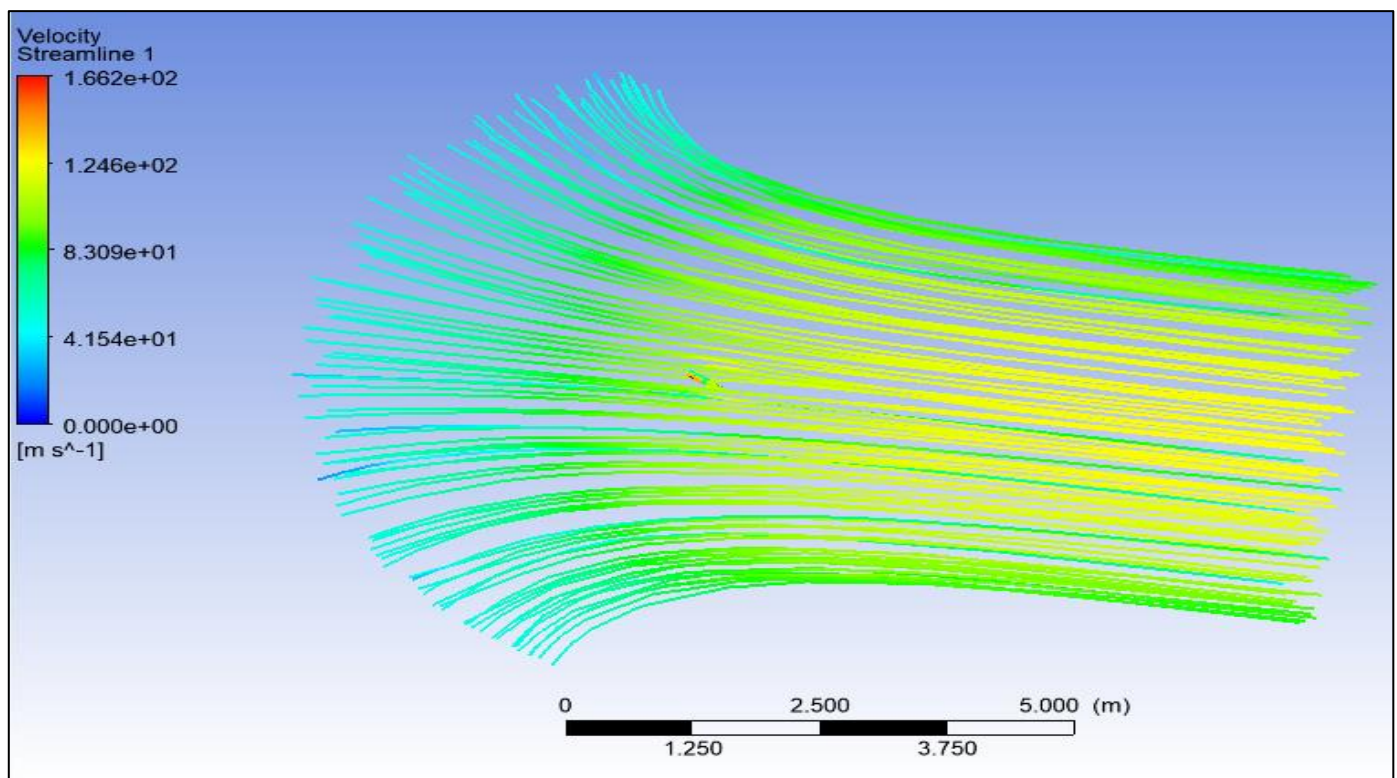


Fig 34: Streamline Velocity Contour Under 15-degree AoA

By increasing the AoA from 10 to 15-degrees, notice how it causes a decrease in streamline velocity to around ~ 166.2 m/s which is more consistent with flow separation (reducing its effectiveness).

- *20° Angle of Attack*

Figure 35 shows the CL in terms of 100 iterations concerning the wing surface when the AoA was adjusted at 20 degree:

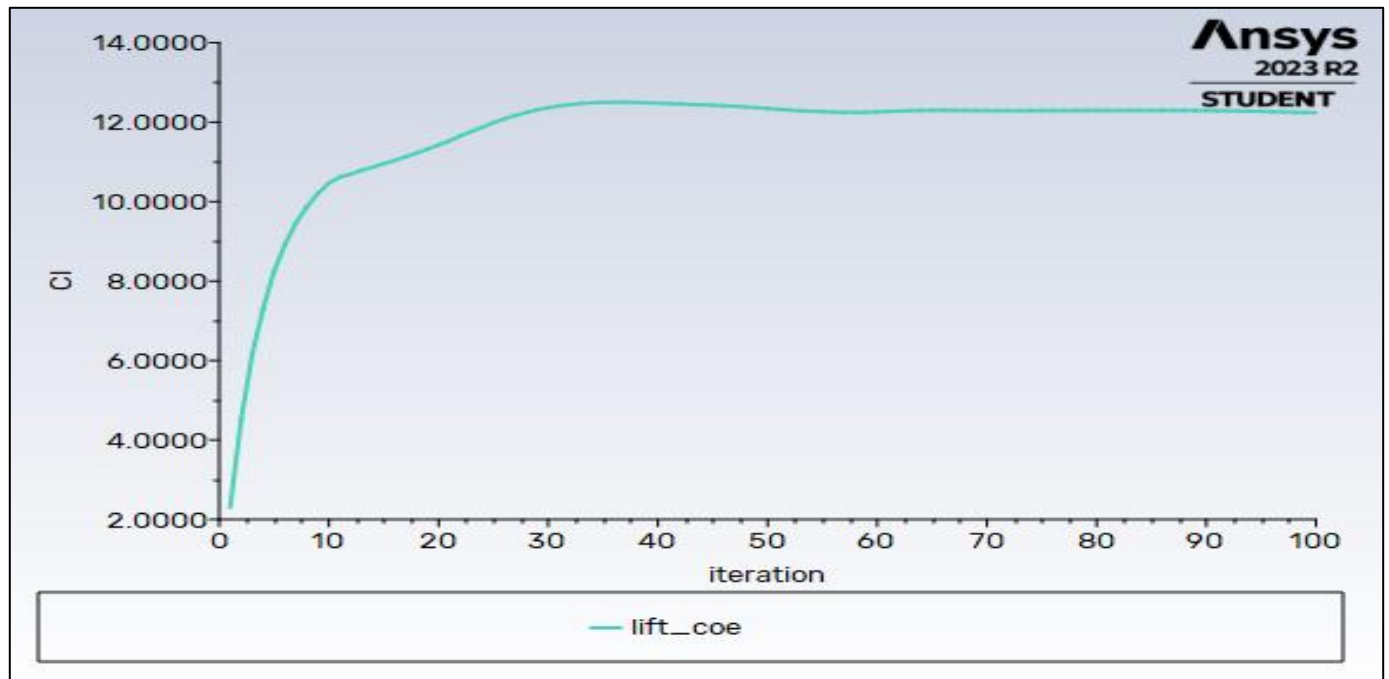


Fig 35: Lift Coefficient Values Under 20-Degree AoA.

It took more than 60 iterations to finally stabilize the lift coefficient. The lift coefficient is 12 when the angle of attack is 20 degrees, as in a. It almost doubles, from 6.5 to 12, so the Angles that give us the biggest lift before the stall is a

reasonable guess. Figure 36 shows the CD in terms of 100 iterations concerning the wing surface when the AoA was adjusted at 20 degree:

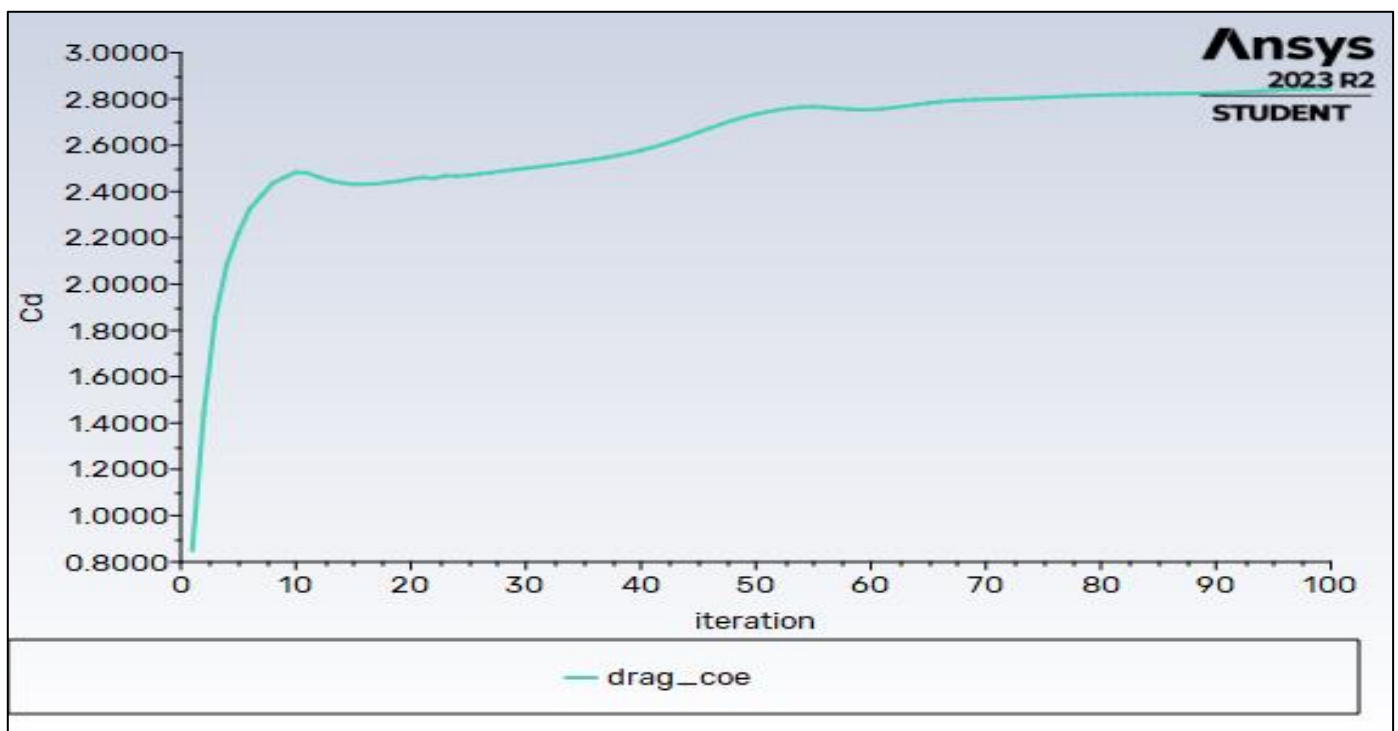


Fig 36: Drag Coefficient Values Under 20-Degree AoA.

Loss convergence coefficients appear to be like as follows from the earlier drag plot, at 80-90 iterations, dropping to a consistent, scaling back to some 2.65. With the drag coefficient at 2.65. The drag coefficient is a measure of how well the limiting potential of the interaction (drag

efficiency) of external air moving over surfaces with a body shape can be obtained. Figure 37 shows the pressure velocity magnitude in terms of contours concerning the wing surface when the AoA was adjusted at 20 degree:

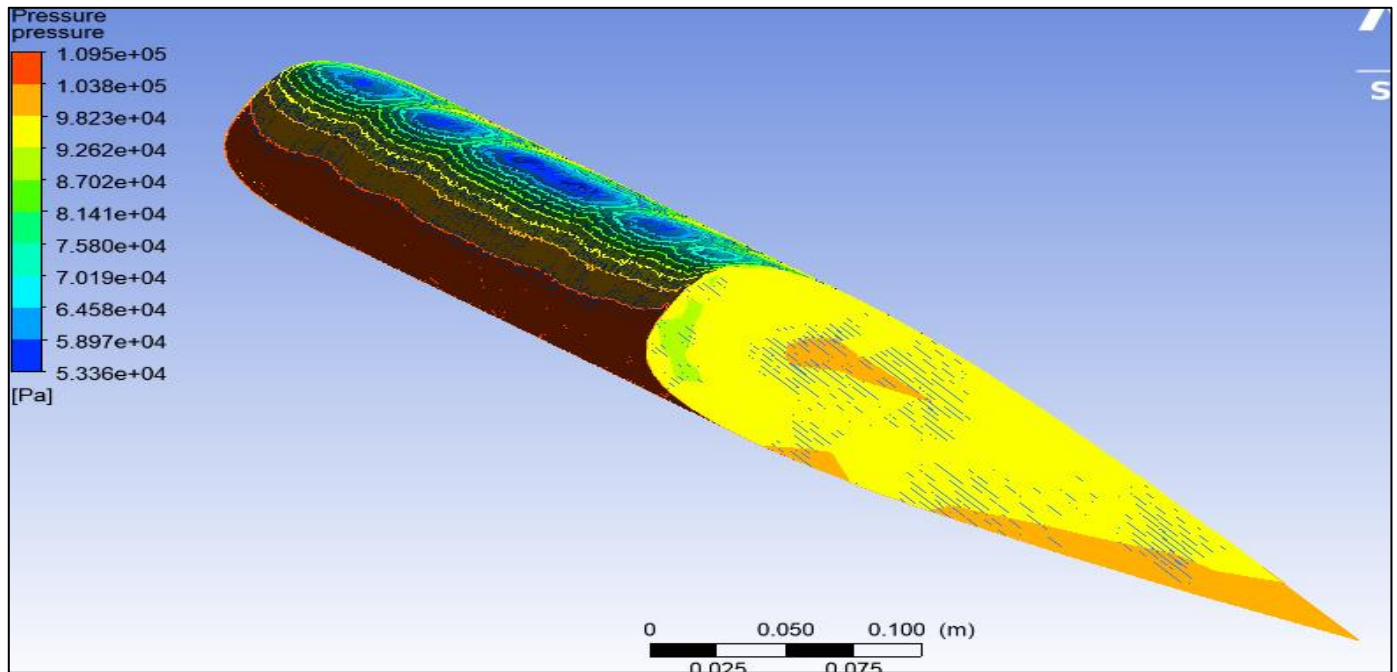


Fig 37: Pressure Contour Under 20-Degree AoA

This case when the AoA was adjusted at 20 degree, the pressure is increased slightly up to 1.095×10^5 Pa. This may be just because of the dynamic response in flow with more lift is generated or because laminar separation bubble

phenomenon occurs. Figure 38 shows the streamline velocity magnitude in terms of contours concerning the wing surface when the AoA was adjusted at 20 degree:

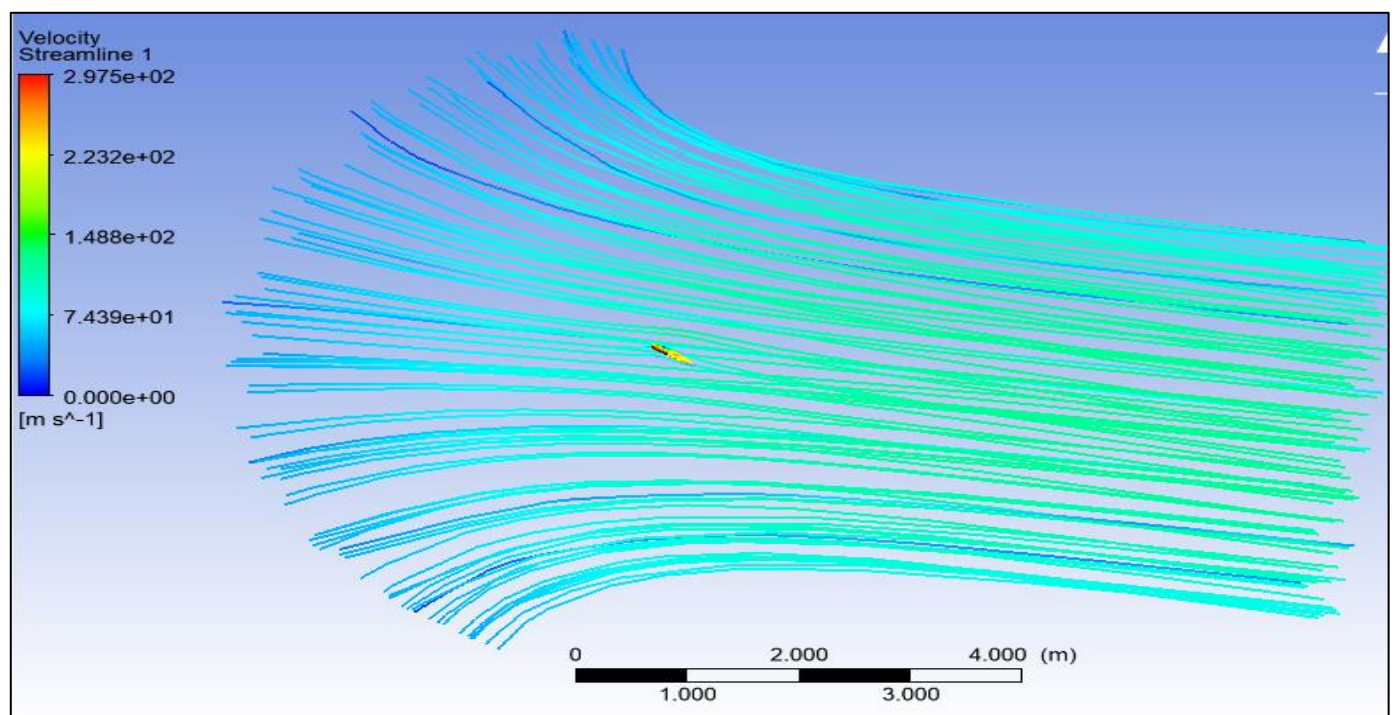


Fig 38: Streamline Velocity Contour Under 20-Degree AoA

The streamline velocity dips dramatically at 297.5 m/s, much as it shown in the figure above; however this sudden drop off is interspersed at these two points and indicates that perhaps some regions where there was massive acceleration of flow owing to possible flow separation, especially on the suction side of each airfoil.

- *25° Angle of Attack*

Figure 39 shows the CL in terms of 100 iterations concerning the wing surface when the AoA was adjusted at 25 degree:

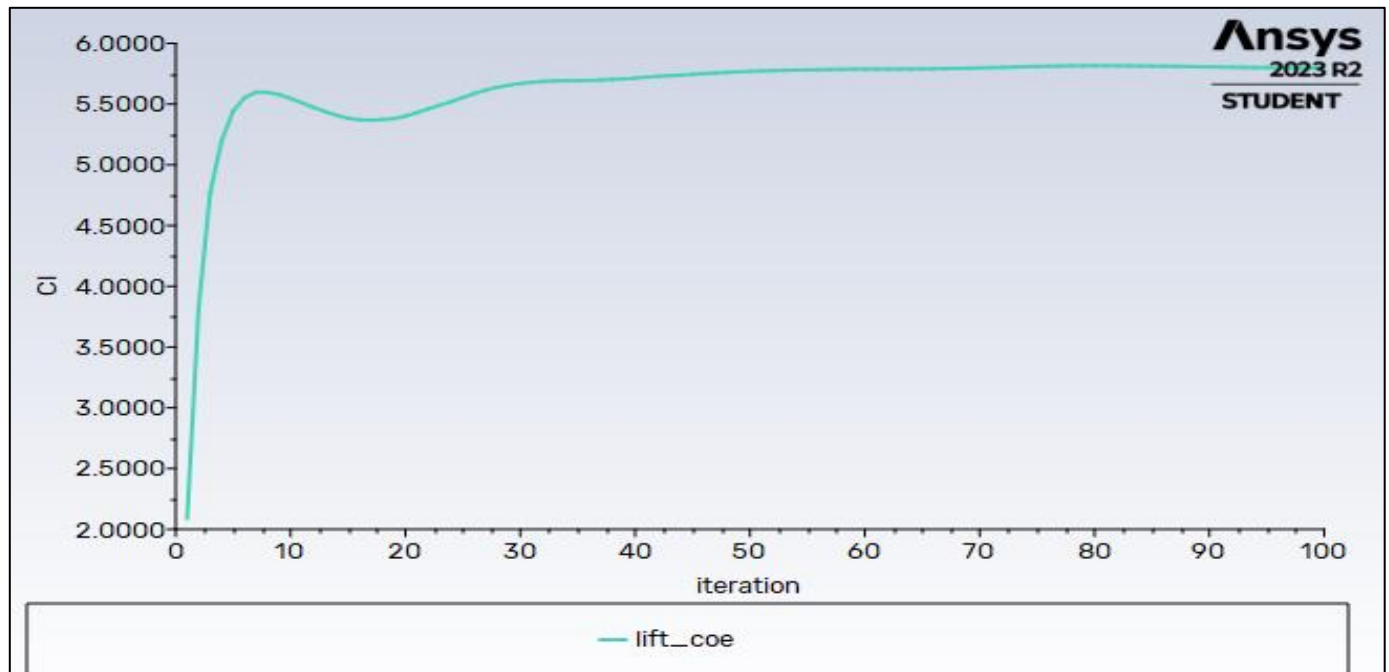


Fig 39: Lift Coefficient Values under 25-Degree AoA

The lift coefficient decreases from 12 to less than 5.5, which marks the onset of stall where separation becomes extensive, and total off-load starts reducing quickly. By the time the CFD simulation have gone through about 45 rounds,

lift coefficient has been converged. Figure 40 shows the CD in terms of 100 iterations concerning the wing surface when the AoA was adjusted at 25 degree:

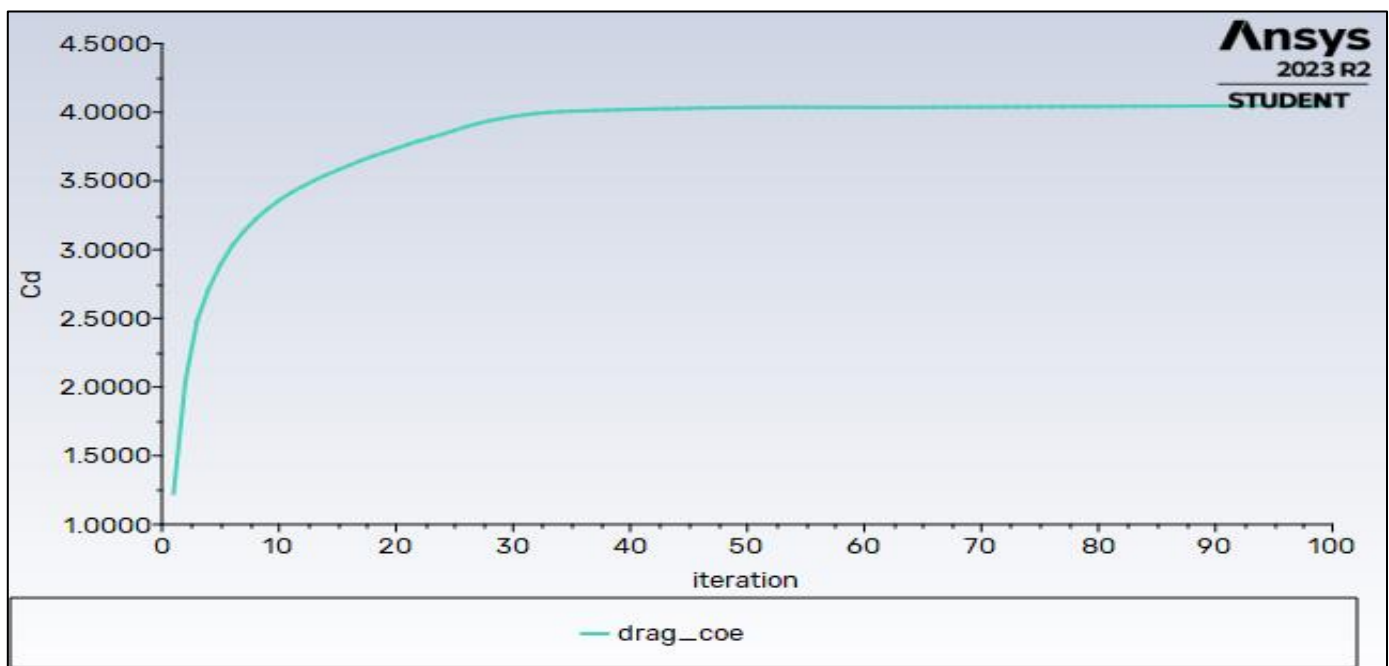


Fig 40: Drag Coefficient Values Under 25-Degree AoA.

In the highest AoA increment, where in this case the drag coefficient increase due to a greater degree of flow separation and turbulence, specifically for drag here (2.65 >> 4). The coefficient of drag is now converged in the range of

45 rounds. Figure 41 shows the pressure magnitude in terms of contours concerning the wing surface when the AoA was adjusted at 25 degree:

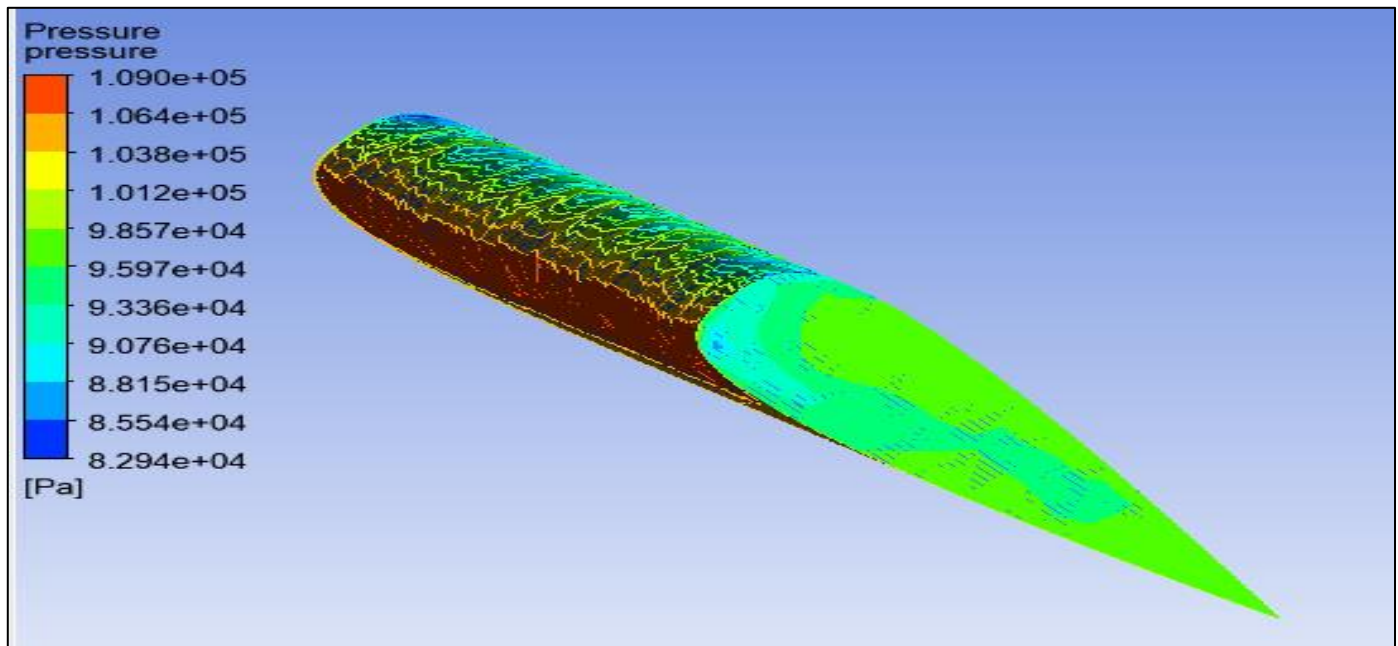


Fig 41: Pressure Contour Under 25-Degree AoA

In the last case, pressure is kept constant at 1.095×10^5 Pa. This regularity indicates that the pressure distribution attains some balance in response to more intense flow

disturbances. Figure 41 shows the streamline velocity magnitude in terms of contours concerning the wing surface when the AoA was adjusted at 25 degree:

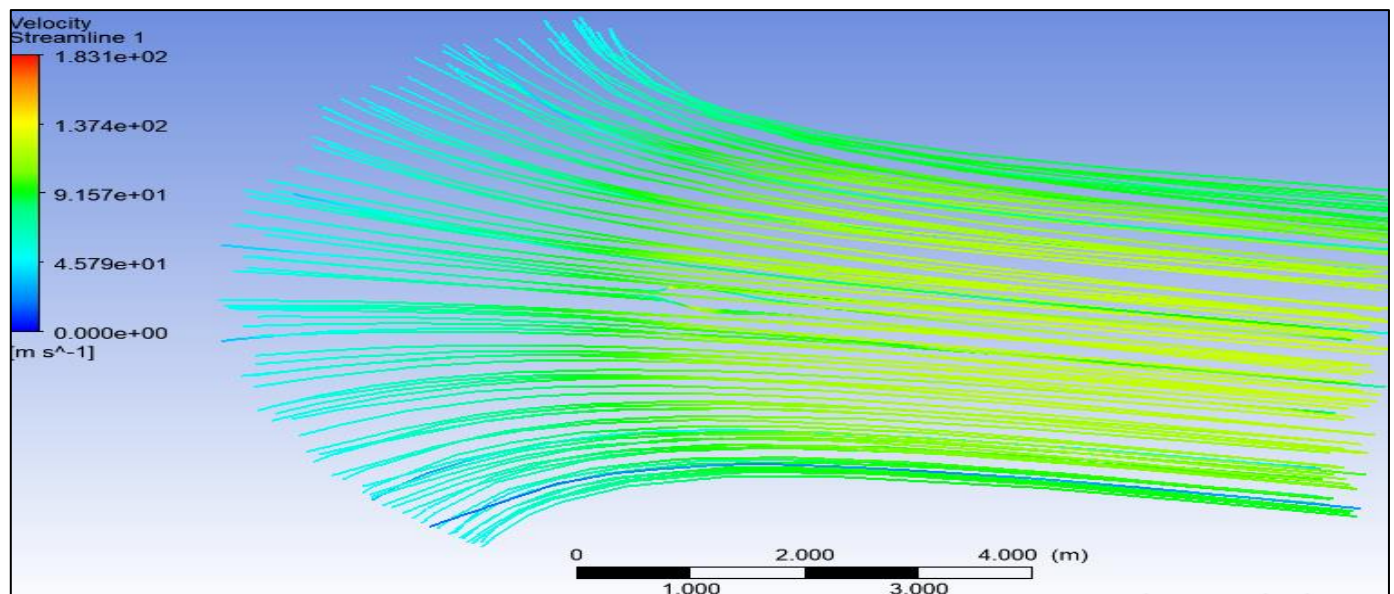


Fig 42: Streamline Contour under 25-Degree AoA

As refers to the contour shown above, the streamline velocity decreases up to 183.0 m/s, imposed by a drastic loss of flow attachment as airfoil angle crosses critical point and streamlined efficiency drops off steeply.

B. Airfoil Performance under AoA Variation

It could be inadequate to just rely on how the plane is designed to create lift; to improve the range of flight, especially with heavy loads, an elevated Cl/Cd ratio must also be achieved. In general, the Cl/Cd ratio is thought to show how efficient an airfoil is. It is the ratio of the airfoil's lift to its drag as it moves through the air. The following table provides a detailed quantitative measure of the aerodynamic

behavior as function of alpha in varying angles for an NACA 0012 airfoil. The data are: pressure, streamline velocity; lift coefficient (Cl), drag coefficient (Cd) and the performance ratio Cl/Cd . This process is vital in examining the effects of varying angles on aerodynamic characteristics of airfoils which plays crucial role for aircraft design and performance enhancement. This data captures how the lift, drag and these forces of each parameter changes as you increase angle of attack from 0° to 15° (on ground effect) in this tradeoff between Lift vs Drag for all these parameters, plus on where has a peaks or critical points that your aerodynamic behavior is at its best or failing.

Table 1: Airfoil Performance Under AoA Variation.

Angle of Attack	Pressure (Pa)	Streamline Velocity (m/s)	Lift Coefficient (Cl)	Drag Coefficient (Cd)	Performance ratio
0	$1.09 * 10^5$	$1.893 * 10^2$	0.001	0.0003	3.33
5	$1.09 * 10^5$	$1.313 * 10^2$	1.86	3.75	0.5
10	$1.092 * 10^5$	$1.747 * 10^2$	6	2.63	2.28
15	$1.087 * 10^5$	$1.662 * 10^2$	6.5	3.25	2
20	$1.095 * 10^5$	$2.975 * 10^2$	12	2.65	4.53
25	$1.095 * 10^5$	$1.83 * 10^2$	5.5	4	1.38

Higher values of pressure generated behind the airfoil, due to faster moving air compared to in front as observed the pressures will remain approximately constant across angles). It is clear from the figure shown above that when airfoil goes through a flow of air, the pressure will slowly rise and show up on the bottom of the airfoil. Bernoulli's principle claims that the airfoil's upper surface has low pressure and its lower surface possesses higher pressure. This means that the flow speeds up on the topmost layer and slows down on the lower surface. The variations can be explained by differing amounts the airflow compresses and expands around the airfoil as it's made to go at different angles of attack.

As the AOA keeps going up and flow separation happens, the Cl/Cd ratio goes down because the lift coefficient drops quickly and the drag coefficient rises quickly. In the case of NACA 0012, CL/CD goes up until the AOA variation method. This is because the top of NACA 0012 does not have any slope and isn't curved as much. So, the flow split at the back edge takes longer than expected.

A pulling effect can be seen at 0 in the NACA 0012 airfoil irrespective of clearance ratios. The reason for this is that a convergent-divergent section forms between the ground and the bottom of the airfoil. By making a venturi flow below the wing, this causes a low-pressure area to form, which leads to negative lift.

As the AOA goes up, the lift coefficient goes up until it hits its highest point (CL max) at 25 degrees, which is additionally referred to as the stall angle. But as the AOA goes up even more, the flow runs into strong opposite pressure gradients that are hard to beat. This causes the flow to split apart and eddies to form. These changes make the flow speed slower and the turbulence stronger on the airfoil's top surface. Because of this, the pressure on top of the airfoil rises, which makes the lift coefficient keep going down.

As the AOA goes up, the flow changes from being smooth to being unstable, which is shown by the change in the drag coefficient within the airfoil. As the turbulence gets stronger, it creates eddies that pull the flow away from the blade surface. This makes the lift coefficient go down and the drag go up, which makes the airfoil not work well. The angle of attack at 20° has the highest performance ratio of 4.53, indicating it is the most efficient in terms of lift versus drag among the tested angles.

V. CONCLUSION

The NACA0012 airfoil's aerodynamic performance was looked at using the CFD software Ansys Fluent at different approach angles (from 0 degrees to 25 degrees) and a constant speed of 50 m/s. To begin searching at the flow through the aerofoil, curves of speeds and pressures were shown. Fluent was used to test CL from all possible attack points. There is more pressure behind the airfoil because the air is going faster than in front of it. As can be seen, the pressures will stay about the same across all angles. The picture above makes it clear that when an airfoil moves by means of a flow of air, the amount of pressure will gradually increase and reveal up on the bottom of the airfoil. Based on Bernoulli's principle, the airfoil's outermost layer has low pressure and the bottom portion has high pressure. In other words, the flow speeds up on the top layer and slows down on the bottom. The trend of the graph showed that as the AoA goes up, so does CL until the flow finally separates. As AoA goes up even more, CL starts to go down. The Cl/Cd ratio goes down as the AOA keeps going up and flow separation happens. This is considering the lift coefficient decreases quickly, and the drag coefficient rises quickly. For NACA 0012, CL/CD goes all the way up to the AOA variation method. The 20° angle of attack has the best performance ratio (4.53), which means it has the most lift compared to drag of all the angles that were tried.

REFERENCES

- [1]. J. E. Allen, "Quest for a novel force: a possible revolution in aerospace," *Progress in Aerospace Sciences*, vol. 39, no. 1, pp. 1-60, 2003.
- [2]. S. Ho, H. Nassef, N. Pornsinsirak, Y. C. Tai and C. M. Ho, "Unsteady aerodynamics and flow control for flapping wing flyers," *Progress in aerospace sciences*, vol. 39, no. 8, pp. 635-681, 2003.
- [3]. J. P. Slotnick, A. Khodadoust, J. Alonso, D. Darmofal, W. Gropp, E. Lurie and D. J. Mavriplis, "CFD vision 2030 study: a path to revolutionary computational aerosciences," 2014.
- [4]. M. H. Khalid, "CFD Analysis of NACA 0012 Aerofoil to Investigate the Effect of Increasing Angle of Attack on Coefficient of Lift and Coefficient of Drag," *Journal of Studies in Science and Engineering*, vol. 2, no. 1, pp. 74-86, 2022.
- [5]. V. Métivier, G. Dumas and D. Poirel, "Aeroelastic dynamics of a NACA 0012 airfoil at transitional Reynolds numbers," In *39th AIAA Fluid Dynamics Conference*, p. 4034, 2009.

- [6]. M. T. S. Khot, "CFD Based Airfoil Shape Optimization for Aerodynamic Drag Reduction (Doctoral dissertation)," 2012.
- [7]. S. S. 365, "Self Study 365," 2018. [Online]. Available: <https://selfstudy365.com/qa/aspect-ratio-in-wings-is-defined-as-5eff00aa7137630d12eb31>. [Accessed 7 2024].
- [8]. J. G. Leishman, "INTRODUCTION TO AEROSPACE FLIGHT VEHICLES," Embry-Riddle Aeronautical University, 2024. [Online]. Available: <https://eaglepubs.erau.edu/introductiontoaerospaceflightvehicles/chapter/airfoil-geometries/>. [Accessed 7 2024].
- [9]. M. A. Malik and F. Ahmad, "Effect of different design parameters on lift, thrust, and drag of an ornithopter," In Proceedings of the world congress on engineering, vol. 2, pp. 1460-1465, 2010.
- [10]. studyflight.com, "Understanding the aerodynamic forces in flight," 2017. [Online]. Available: <https://www.studyflight.com/understanding-the-aerodynamic-forces-in-flight/>. [Accessed 7 2024].
- [11]. B. W. McCormick, Aerodynamics, aeronautics, and flight mechanics, John Wiley & Sons. 1994.
- [12]. myassignmenthelp.net, "Stability and control," 2007. [Online]. Available: <https://www.myassignmenthelp.net/sample-assignment/stability-and-control>. [Accessed 7 2024].
- [13]. M. McCarty, "The Measurement of the Pressure Distribution over the Wing of an Aircraft in Flight," Thesis, School of Aerospace, Civil and Mechanical Engineering, University of New South Wales, Australia, 2008.
- [14]. S. A. Shafi, "Civil aero-propulsion application: effect of thrust rating change on engine time on-wing," CRANFIELD UNIVERSITY, 2015.
- [15]. S. Nawrin, "CFD ANALYSIS OF AERODYNAMIC PERFORMANCE OF NACA 0018 AIRFOIL CONSIDERING SUCTION AND INTERNAL SLOT," SCIENCE IN MECHANICAL ENGINEERING, 2021.
- [16]. P. Mancini, "Experimental investigation into unsteady force transients on rapidly maneuvering wings," University of Maryland, College Park, 2017.
- [17]. M. McCarty, "The Measurement of the Pressure Distribution over the Wing of an Aircraft in Flight," UNSW Sydney, 2008.
- [18]. M. Sadraey and D. Müller, "Drag force and drag coefficient. M. Sadraey, Aircraft Performance Analysis," VDM Verlag Dr. Müller. 2009.
- [19]. I. H. Abbott and A. E. Von Doenhoff, "Theory of wing sections: including a summary of airfoil data," Courier Corporation., 2012.
- [20]. S. P. Sane and M. H. Dickinson, "The control of flight force by a flapping wing: lift and drag production," Journal of experimental biology, vol. 204, no. 15, pp. 2607-2626, 2001.
- [21]. R. Groh, "Boundary Layer Separation over the Top Surface of a Wing," Aerospace Engineering Blog, 2016.
- [22]. T. C. J. Cousteix and J. Cebeci, "Modeling and computation of boundary-layer flows," Berlin, Germany: Springer, 2005.
- [23]. İ. Göv and M. H. Doğru, "Aerodynamic optimization of NACA 0012 airfoil," The International Journal of Energy and Engineering Sciences, vol. 5, no. 2, pp. 146-155, 2020.
- [24]. D. H. Kim, J. W. Chang and J. Chung, "Low-Reynolds-number effect on aerodynamic characteristics of a NACA 0012 airfoil," Journal of aircraft, vol. 48, no. 4, pp. 1212-1215, 2011.